Electrochemical Oxidation Coupled with Anaerobic Digestion for Sustainable Microalgae Cultivation Media: Upcycling Food Biomass

陳, 海博

(Degree)
博士（農学）

(Date of Degree)
2024-03-25

(Date of Publication)
2025-03-01

(Resource Type)
doctoral thesis

(Report Number)
甲第8946号

(URL)
https://hdl.handle.net/20.500.14094/0100490171

Doctoral Dissertation

Electrochemical Oxidation Coupled with Anaerobic Digestion for Sustainable Microalgae Cultivation Media: Upcycling Food Biomass

（電気化学的酸化と嫌気性消化を組み合わせた持続可能な微細藻類培養培地:食品バイオマスの創造的再利用）

January, 2024

Graduate School of Agricultural Science,
Kobe University

HaiBo Chen (陳 海博)

Acknowledgments

Throughout the writing of this dissertation, I have been greatly supported and assisted.

I would especially like to thank my supervisor, Professor Ikko Ihara, for guiding me in the right direction to successfully complete my dissertation. He provided insightful feedback that pushed me to sharpen my thinking and take my work to a higher level, for which I am enormously grateful. In addition, I would like to thank Professor Gen Yoshida for his valuable advice and help, whose research methods greatly improved the results of my research.

I would also like to express my gratitude to the members of the team, Fetra J Andriamanohiarisoamanana and Keita Inagaki, for their wonderful collaboration and patient support on the anaerobic digestion and microbial cultivation experiments. They have provided me with experimental skills on many occasions. I would also like to thank Professor Hiromichi Itoh and Professor Koichi Shoji, they greatly helped me to polish my dissertation. I appreciated the support received from Mohamed Ramadan, who polished my first draft of the dissertation. Without them, this dissertation would never have been completed.

Finally, I would like to acknowledge the support of my family and friends during the completion of this dissertation. They have provided me with delightful distractions to keep me occupied outside of my studies.

Catalog

List of Tables

List of Figures

Chapter One
Exordium

1.1 Background

Growth and production of commodities and food in modern society involve large-scale industrial and agricultural activities. In addition to the desired products, these activities also produce large quantities of waste that can cause serious environmental problems if it is not properly managed. As a result, in order to save energy and resources, the concepts of recovery, recycling and reuse have been the mainstream in the modern world especially in industrial processes.

Dark-colored food waste is generated from food industries such as coffee producing process, soy sauce, can, beverage production and yeast, liquor ethanol manufacturing with molasses. Anaerobic digestion is one of the most cost-effective processes to treat food waste. Both the food waste and anaerobic digestate, are dark in color and also characterized by a high concentration of organic biomass (e.g., protein, saccharides, aliphatic and aromatic compounds) and inorganic materials (e.g., ammonium, phosphorus, sulfur and potassium). Based on the significant amount of organic matter and inorganic matter in the food waste and anaerobic digestate, it is necessary to develop cost-effective treatments that are dedicated to decolorizing dark colors and allowing reuse of the valuable matter for food production like cultivation of edible photosynthetic microalgae.

1.2 Addressed Issues in this Research

This study investigated the decolorization of acid orange 7 (AO7), caramel, and liquid digestate from food biomass waste by electrochemical oxidation (EO) with boron-doped diamond (BDD) anodes. For the reuse of nutrients that remained in the effluent of food biomass food waste, the decolorized liquid digestate was used as a medium for microalgae cultivation, and the results of the cultivation were available as expected in the experiments.

Overdosage use of colorants such as food colorants caramel in food industries has caused severe environmental problems including greenhouse gas run-off, waterbody eutrophication, and nutrients leaching into the ground. In the first work, the EO combined with electro-Fenton (EF) process using BDD electrodes was applied as an effective treatment for color removal and achieved a significant decolorization of caramel colorants. It highlighted the potential of EO combined with EF (EO+EF) process using BDD electrodes for efficient degradation of caramel colorants.

Moreover, to reach the modern ecological strategy, treated effluents should be recycled and reused to save and make full use of energy and resources. Anaerobic digestion is one of the most appropriate technologies to treat food biomass wastes. Anaerobic digestate is the effluent from anaerobic digestion, it generally contains abundant nutrients. Although the direct discharge of digestate onto local croplands is the simplest disposal, it has limitations of processing capacity and potential risk to the ecosystem. In recent years, the combination of digestate treatment and microalgae cultivation of biomass has been considered as an ideal strategy for the resource recovery of food biomass waste and digestate. However, the digestate generally involves a high level of turbidity, which hinders light permeation into the medium. Therefore, in the second work, the EO process using a BDD anode promoted the decolorization of liquid digestate and retained most of nutrients, especially the ammonium-nitrogen (NH_4-N). The decolorized liquid digestate has the potential to be used as an appropriate medium for microalgae cultivation. In Chapter 4, the experiments proved that

the electrochemically oxidized liquid digestate as a highly light-permeable medium, improved the growth performance of *C. sorokiniana* cultivation, compared with the liquid digestate medium.

1.3 Research Objects

In this research, the general and main object is to save and take full advantage of energy and resources corresponding with the ecological system. To reach this goal, investigations of effective decolorizations, anaerobic digestions, microalgae cultivations, and their optimizing conditions have been implemented. They consist of the following minute processes.

1) The removal of caramel colorants from effluents of liquid food waste using an EO+EF process with BDD electrodes. EO, EF and EO+EF processes were applied to decolorize colorants. Caramel is a representative food colorant, especially in coffee products and it is persistent and refractory for decolorization. For comparison, one of the most typical azo dyes, AO7, was used in the electrochemical decolorization of food colorants. This dissertation compared different decolorization methods for caramel and AO7 using BDD anodes and Ti/Pt anodes. The effects of air flow rate for oxygen supply, initial concentration of added Fe^{2+}, and applied current on decolorization were evaluated and energy consumption was analyzed.
2) The treatment of liquid digestate from food waste biomass by an EO process to produce a light-permeable medium for microalgae cultivation. An anaerobic liquid digestate from coffee waste biomass and another kind of typical digestate from dairy cow manure were compared to investigate their decolorization properties. The electrochemical decolorization of the spent coffee grounds liquid digestate was compared with that of dairy cow manure liquid digestate. The effects of anodic material, initial Fe^{2+} concentration, and current on electrochemical decolorization were evaluated and changes in the nutrients in the digestate were investigated and energy consumption was analyzed.
3) The cultivation of *Chlorella sorokiniana* NIES-2173 using a medium of electrochemically

oxidized liquid digestate from coffee waste biomass. The decolorization performance of digestates, changes in the nutrients, and chemical oxygen demand (COD) removal were evaluated. The effects of dilution of liquid digestate and the reaction time of electrochemically oxidized liquid digestate on microalgae cultivation were also investigated and energy consumption was analyzed.

Through these investigations, the dark-colored liquid digestate from coffee waste biomass treated with the EO process using BDD anodes is a better medium for microalgae cultivation than with non-treated liquid digestate.

Dark-colored food waste is generated from the food industry, such as the coffee production process. Caramel is a representative but persistent and refractory food colorant and it is commonly used in coffee products. Coffee waste biomass is a potential substrate for anaerobic digestion, whereas it also remains dark color such as the caramel. Therefore the electrochemical decolorization which is effective in decolorization of caramel is necessary for producing a highly light-permeable medium. Fig. 1-1 shows the graphical abstract, including a flow diagram of the three contributed papers. From the investigation of electrochemical decolorization of caramel colorants in coffee products, to verifying the feasibility of the coffee waste liquid digestate treated by electrochemical decolorization, and finally, the trial of microalgae cultivation using the electrochemically oxidized liquid digestate as a medium, the whole research proved that the EO process is feasible to decolorize colorants in coffee products and coffee waste liquid digestate, and the product is a highly light-permeable medium with nutrients for microalgae cultivation.

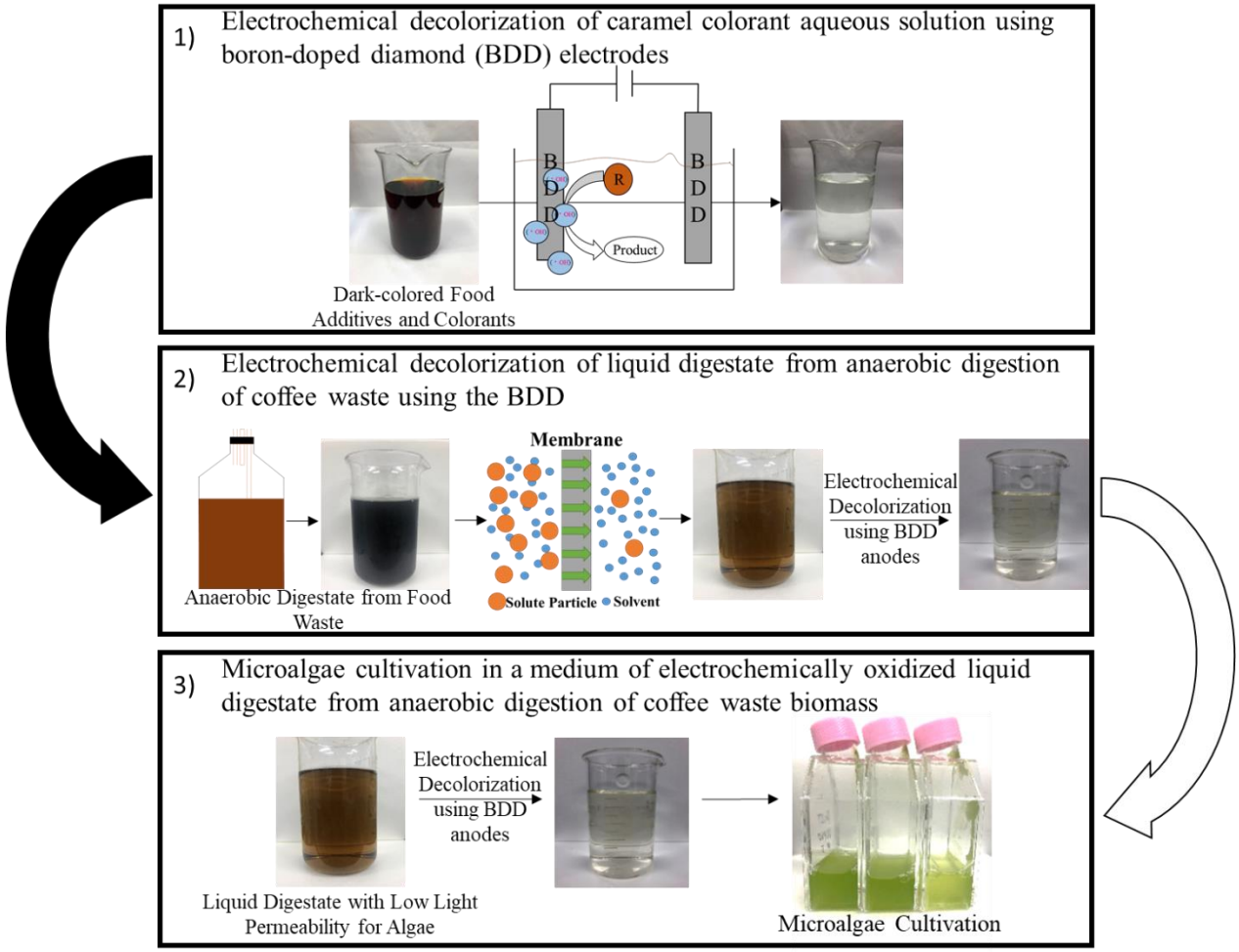

Fig. 1-1 Graphical Abstract

1.4 Constitutions

This paper consists of six chapters, the abstract of each chapter was presented as follows:

Chapter 1: the main object of food waste biomass recovery, recycling and reuse. The background introduces the necessity and reason that is carried out in this research. The achievements and addressed issues prove that the work contributed to the main object.

Chapter 2: the situation of food waste biomass recycling and reuse, including the unsettled issues or problems caused by colored matter and their promising disposals and treatments.

Chapter 3: the effects of the EO+EF process using BDD electrodes on the decolorization of widely used and biorefractory food colorant caramel.

Chapter 4: the effect of electrochemical decolorization of liquid digestate from coffee waste biomass using BDD anodes to produce a light-permeable medium for microalgae cultivation.

Chapter 5: microalgae cultivation using a medium of electrochemically oxidized liquid digestate from coffee waste biomass.

Chapter 6: the summarized results according to all foregoing contents, the ending conclusion comes out in this chapter.

Chapter Two

Previous Researches

2.1 Colorants

2.1.1 A wide use of colorants

Colorants or pigments or dyes, they are referring to the same content concerning dyeing the given color on object things. A wide variety of colorants have been used in industrial processes such as Ponceau 4R, Sunset Yellow FCF, Reactive Yellow HF, Reactive Black 5, Orange II, AO7, Acid Red 151, Direct Blue 71, Reactive Yellow 160, Methyl Orange, and the azo dye is the main part (70% of the world dye production) (Garcia-Segura et al., 2011a) in colorants use. Such colorants generally are applied in tannery, textile, oil paint, paper, and food production processes. However, large-scale applications caused large quantities of discharge into the environment, and the azo dyes are very stable and biorefractory in the environment owing to their persistence under natural redox conditions, sunlight exposure, and biodegradation (Martínez-Huitle & Brillas, 2009).

2.1.2 Food colorants

As a main part of colorants, food colorants are important additives or by-products in food industries. The generally used food colorants include azo dyes of Allura Red, Brilliant Black BN, Brown HT, Ponceau 4R, Sunset Yellow FCF (Yamjala et al., 2016), and complex pigments of molasses, melanoidins, and caramel. Melanoidins are generically defined as high molecular weight nitrogenous dark brown colored compounds (Moreira et al., 2012). Caramel colorant is a complex mixture of separable high and low-molecular-weight constituents (Tomasik, 2003). They are widely used in sweetmeats, pastries, condiments (soy sauce and dressing), and beverages (especially in colas and canned coffee). In modern society, the mass production of them is because they polish food to make a finishing point, involved with special taste and pleasant color.

2.1.3 Current treatments for colorants

Various treatments have been applied to treat effluent containing the colorants, including physical and/or physicochemical treatment and biological treatment. For example, adsorption with activated carbon has been utilized for melanoidin decolorization (Simaratanamongkol & Thiravetyan, 2010) and discoloration of caramel from sugar cane juice was obtained through ultrafiltration coupled with ion exchange decolorization process (Susanto et al., 2016). In the study of Santal et al. (2011), melanoidin food colorant could be biodecolorized by aerobic bacterial strain SAG_5. Although physical and/or physicochemical methods achieve available decolorization yield, inevitably they generate large volumes of sludge (Ahmad et al., 2017) and require regular maintenance of absorbent or membrane (Garcia-Segura et al. 2011b; Bedolla-Guzman et al. 2016).

Moreover, some recalcitrant colorants, like caramel, are biorefractory and difficult to be degraded with non-destructive methods (Özcan & Özcan, 2018) in the effluents of each processing.

Electrochemical advanced oxidation processes (EAOPs) as an intensive treatment that can directly and/or indirectly oxidize organic matter, have drawn great attention in recent decades. One of them, EO is a simple and widespread EAOP because it always has a high removal efficiency using a simple apparatus under mild conditions (Thiam et al., 2016). In the EO process, electrons are generated or consumed without certain chemical side products which often occur in other treatments (Krzemińska et al., 2015).

The EO process is used in the sugar industry, some typical colorants like molasses and melanoidins generated from the sugar production process were decolorized effectively by an EO (Sahu & Chaudhari, 2015). As for the azo dye, methyl orange was decolorized by an EO using a Ti_4O_7 anode (Wang et al., 2020).

Electro-Fenton process is a vital EAOP, it refers to EO based on Fenton reaction chemistry, which degrades organics using Fenton's reactions (Brillas et al., 2009). Fenton's reactions are mainly

composed of Fenton reagents which consist of Fe^{2+} and H_2O_2. Fenton reagents proceed a reaction of generating ·OH, a sort of strong oxidant with non-selective oxidation of most organic matter, and attaining Fe^{3+}, according to reaction (2-1) (Neyens & Baeyens, 2003):

$$Fe^{2+} + H_2O_2 \rightarrow Fe^{3+} + \cdot OH + OH^- \quad (2\text{-}1)$$

In the EO process, most cathodes and cathodic reactions generate H_2O_2 by reaction (2-2):

$$O_2 + 2H^+ + 2e^- \rightarrow H_2O_2 \quad (2\text{-}2)$$

To some extent, the generated H_2O_2 by the cathode and regenerated Fe^{2+} by the anode (Fe^{3+} to Fe^{2+}) achieve a circular reaction including Fenton reactions.

2.1.4 The colorants in coffee products

To meet the aesthetical requirements or special demands, dying with colorants is becoming an indispensable procedure in modern food production processing. Except to meet the special demands on purpose, every raw material has its original color. Additionally, some colorants are generated inevitably during the processing like aerobic fermentation and anaerobic digestion such as humus and fulvic acid-like compounds from metabolic reactions (Monlau et al., 2015), and heating processing such as melanoidins from Maillard Reaction (Tomasik, 2003), Caramel from Caramelization (FAO, 2011). The fermentation and roasting processing is necessary for most kinds of coffee raw materials (Mussatto et al., 2011). It means that the colorants are everywhere throughout the industrial processing, nearly all of the coffee products contain colorants, except the inevitable color, and even large amounts of additional colorants are added artificially.

2.2 Coffee waste biomass

2.2.1 The effluent of coffee waste

Coffee is one of the most popular beverages consumed in the world and the second-largest traded commodity after crude oil (Murthy & Madhava Naidu, 2012). Global coffee consumption continued steady grow steadily annually. According to the International Coffee Organization's and United States Department of Agriculture's statistics (USDA, 2023), the annual consumption of coffee worldwide reached 10.1 million metric tons in 2022. As a solid residue from the brewing of the most renowned drink worldwide, coffee, almost 90% of the weight quantity of coffee consumption was discarded after use as spent coffee grounds. The organic components presented in coffee pulp involve cellulose (63%), lignin (17%), proteins (11.5%), hemicelluloses (2.3%), tannins (1.80–8.56%), pectic substances (6.5%), reducing sugars (12.4%), non-reducing sugars (2.0%), caffeine (1.3%), chlorogenic acid (2.6%) and caffeic acid (1.6%) (Mussatto et al., 2011).

The term instant or dissoluble coffee is defined as the powder or granules that remain after water drains from the coffee solution. The production of instant coffee generally started with grain roasting. This procedure allowed the formation of special sugars and the characteristic dark brown color of coffee (Rodrigues & Bragagnolo, 2013). Generally, it can be used to produce canned coffee. The dissolution of coffee powder with water, which is a crucial procedure in the production of coffee flavor beverages and canned coffee, generates large amounts of coffee waste effluent including coffee powder waste (spent coffee grounds). The composition of coffee waste effluent includes a mixture of complex compounds, such as high molecular weight molecules like proteins and polysaccharides. Other complex substances that are contained in the coffee waste effluent are caramel, melanoidins, caffeine, and tannins (Rigueto et al., 2020). Many environmental issues associated with coffee waste

effluent include water eutrophication, toxicity to aquatic creatures and plants, soil salinization overgrowth of microbes and insects, and generation of foul odors (Kulandaivelu & Bhat 2012; Woldesenbet et al., 2014). Therefore, more sustainable and environmentally friendly treatment options were indispensable to lower the negative effect of the current treatment of coffee waste effluent on the environment.

2.2.2 Treatments of coffee waste biomass

Coffee waste biomass has been studied for the production of activated carbon, biodiesel, and anaerobic digestion (Caetano et al., 2014). Although the coffee waste biomass contains various valuable organic matter and nutrients as many previous researches mentioned, owing to the cost of disposal, till now, most of the spent coffee grounds have been merely incinerated (Zhang et al., 2021). It's worth mentioning that this way of disposal of the spent coffee grounds is not friendly to the ecosystem. Many treatments with high recycling ratios can be options, anaerobic digestion has overt potential advantages and the biogas generated from the anaerobic digestion of organic matter can be applied as renewable energy.

2.3 Anaerobic Digestion

2.3.1 Anaerobic digestion of coffee waste biomass

One of the most promising technologies for treating organic effluents and biomass processing residues is anaerobic digestion. Metabolic reactions, successively the hydrolysis, acetogenesis/acidogenesis, and eventually methanogenesis processes mainly comprise anaerobic digestion. These processes aim to promote the microbial biodegradation of organic compounds and generate different molecules and precursors of bioenergy (Pinto et al., 2018). Anaerobic digestion has been verified to be a promising treatment for the valorization of organic matter such as agricultural wastes (coffee waste products, crop residues, and manure), food waste biomass, and sewage sludge (Moretti et al., 2020). Based on previous researches, the reuse of spent coffee grounds as raw substrates for anaerobic digestion and biogas production presented great potential.

From the point of Luz et al. (2017), spent coffee grounds are a biomass that needs less pre-treatment, is rich in nutrients, and can be easily separated by coffee machine in situ, This indicates that the spent coffee grounds have great potential for use as a substrate for anaerobic digestion. Lane (1983) and Girotto et al. (2018) also clarified the feasibility of coffee waste including spent coffee grounds for anaerobic digestion. Vítěz et al. (2016) show that coffee waste has high biotechnical value with the presence of polysaccharides, proteins, and minerals as a substrate which can be used for the fermentation process. In summary, the previous research clarified that anaerobic digestion converted coffee waste biomass into biogas efficiently and generated digestate.

2.3.2 Treatments of digestate from coffee waste digestion

Anaerobic digestate is the effluent from anaerobic digestion. Anaerobic digestate usually involves large contents of mineralized nutrients such as N and P, and a great amount of insoluble particles (Mucha et al., 2019) during anaerobic digestion of coffee waste. Anaerobic digestate from anaerobic digestion is more appropriate as a renewable alternative to conventional mineral fertilizers in practices of agricultural land (Monlau et al., 2015). However, some environmental risks related to the land application of liquid digestate in the fertilizing field, including heavy metals into the soil, deterioration of the landscape, phytotoxicity of digestate, proliferation of pathogens, and attraction of pests (Albiach et al., 2000; Sánchez-Monedero et al., 2004) need more attention. Aerobic biofilters and dissolved air flotation of the aerobic process have been used to further treat anaerobic digestate. Although the N, P nutrients, and organic matter contained in the anaerobic digestate can be reduced effectively, a series of aerobic processes generate a large amount of CO_2 and excess sludge which requires further disposal (Huo, et al., 2018). Additional nutrient recycling processes are required following anaerobic digestion to achieve effective nutrient reuse (Tian et al., 2018).

Apart from conventional land applications and aerobic processes, phytoremediation like microalgae cultivation with anaerobic digestate has been validated. Sayedin et al. (2020) used thin stillage digestate for nutrient recovery by microalgae cultivation. Rajagopal et al. (2021) applied liquid digestate from poultry for microalgae bioproducts and Kisielewska et al. (2022) used liquid digestate from maize silage for biomass production.

2.4 Microalgae Cultivation

2.4.1 Applications of microalgae

The term microalgae refers to algae that are too minute to be visible to the unaided eye. The major taxonomic orders of algae involve Chlorophyta (green algae), Chrysophyta (golden algae), Rhodophyta (red algae), and Bacillariophyta (diatoms) (Stengel et al., 2011). Microalgae have been studied in the treatment of various wastewaters, including palm oil mill effluent (Hadiyanto et al., 2013), rubber mill wastewater (Bich et al., 1999), textile wastewater (Lim et al., 2010) and even wastewater with heavy metals (Aksu, 2001). Microalgae have strong robustness making them thrive even in extreme conditions and this is also a merit to treating wastewater.

Microalgae can take advantage of nitrogen and phosphorus nutrients from liquid digestate and CO_2 that are sufficient in the atmosphere (Beuckels et al., 2015). Large amounts of sugar, fatty acid and other valuable byproducts can be accumulated in the microalgal cells. Owing to their easy production, short life cycle, rapid growth rate, high efficiency of photosynthesis, and independence from conventional soil land, microalgae have great potential in future industrial applications (Rahman, 2019). Biomass of microalgae has long been recognized as a high-value product for biofuels (Raheem et al., 2018), feed (Spolaore et al., 2006), nutrition, cosmetic productions, and especially as a kind of high-value food additive for humans, because of its high content of protein, high amounts of vitamins, antioxidants, and other valuable bioactive compounds (Huo et al., 2018).

2.4.2 Anaerobic digestate used in microalgae cultivation

In recent years, the combination of digestate treatment and microalgae biomass production has been considered as a potential method for the resource recovery of anaerobic digestate. The treated digestate can be a medium for microalgae cultivation. Anaerobic digestate like dairy manure (Wang et al., 2010) and thin stillage digestate (Sayedin et al., 2020) are used for nutrient recovery by microalgae cultivation. Liquid digestate such as liquid fertilizer PAL1 (Dang & Lee, 2018), sewage sludge (Sekine et al., 2020), poultry liquid digestate (Rajagopal et al., 2021), and maize silage liquid digestate (Kisielewska et al., 2022) is applied for microalgae bioproducts and biomass production. Although these combined methods have the potential to reduce the cost of wastewater treatment and generate valuable microalgal biomass, many issues restrict the application of these treatments. One of the most typical restrictions on the use of liquid digestate as a medium for microalgae cultivation is the low light permeability of liquid digestate.

2.4.3 Pre-treatment of the digestate as a medium

Anaerobic digestate contains large amounts of insoluble particles contributing to high turbidity, which hampers the light penetration into the medium (Mohd Udaiyappan et al., 2017). Meanwhile the dark brown to black compounds such as soluble microbial byproducts, humic acid-like and fulvic acid-like matter, deeply dye the anaerobic digestate (Wang et al., 2019), which is not conducive to the photosynthesis of microalgae. Consequently, the turbidity of suspending solid (SS) removal and decolorization of liquid digestate become a priority for microalgae cultivation using an anaerobic digesate medium.

Different methods have been evaluated for decolorizing the anaerobic digestate. Precipitation (Chen et al., 2012), microfiltration (Bchir et al., 2011), and centrifugation (Franchino et al., 2013) are applied to remove turbidity, mainly the insoluble SS in liquid digestate. The liquid digestate without SS has higher light permeation. However, the liquid digestate remains dark because of the soluble, colored organic compounds. Moreover, color removal by absorption requires subsequent activated carbon, which is pricy and time-consuming (Huo et al., 2021). Therefore, a more appropriate and adequate decolorization process is in demand.

2.4.4 Electrochemical decolorization of the digestate

In summary, the EO process can effectively decolorize colorants from wastewater. Therefore, some researchers intend to use EO as a decolorization process for treating anaerobic digestate. The EO has been used as a final step to decolorize the remaining olive mill wastewater fraction from an anaerobic reactor (Gonçalves et al., 2012). In decolorization by EO, electrochemically generated hypochlorite has been used from chloride ions in solution (Martínez-Huitle et al., 2015). This production of hypochlorite by the electrochemical reaction reduces the concentration of NH_4-N, which is a nutrient source for algae. For example, when liquid digestate from the anaerobic digestion of dairy manure was treated by EO with a dimensionally stable anode (DSA) based on mixed oxides of RuO_2 + IrO_2, the NH_4-N concentration decreased because of electro-generated hypochlorite (Ihara et al., 2006).

The selection of an appropriate anode material is important for the EO process. As an electrode, BDD provides a high overpotential for oxygen production and a wide potential window. Because of these properties, rather than generating and using hypochlorite, BDD anodes generate ·OH and use it to oxidize organic compounds (Panizza & Cerisola, 2005). The EO process using a BDD anode (EO-BDD) has been applied to the decolorization of dark solutions, such as those colored with melanoidins (Liakos et al., 2017) and the synthetic azo dye Ponceau 4R (Thiam et al., 2016). In these applications, hydroxyl radical (·OH) is likely the primary active species instead of hypochlorite. Therefore, the liquid digestate decolorized by the EO using BDD anodes can be a promising medium for microalgae cultivation.

Chapter Three

Electrochemical decolorization of caramel colorant aqueous solution using BDD electrodes

This paper was published in the Journal of Water Process Engineering (Chen et al., 2022)

3.1 Introduction

The electrode is a vital parameter when improving the efficacy of electrolytes as the mechanism and the products of anodic reactions are known to critically depend on the anode material (Liakos et al., 2017). BDD electrode is found to be appropriate for electrochemical applications owing to its high activity towards ·OH production and other characteristics, including chemical inertness, high hardness, wide electrochemical window, and electrochemical stability (Panizza & Cerisola, 2005).

$$BDD + H_2O \rightarrow BDD(\cdot OH) + H^+ + e^- \quad (3\text{-}1)$$

EO coupled to EF process for dye effluent treatment has been reported previously. However, most of these coupling processes are carried out one after another (i.e. as a pre-treatment to a post-treatment) (Wang et al., 2020). Few studies have shown the simultaneous application of EO and EF in a synergic electrochemical system, and the BDD had much greater oxygen evolution overpotential than other conventional anodes (Pereira et al., 2016). Therefore, as a non-active anode, BDD can generate physisorbed BDD(·OH), a variety of strong oxidants, at the BDD anodic surface through reaction (3-1) (Thiam et al., 2016) for the EO process. As a cathode, the BDD cathode continuously feeds H_2O_2 into contaminated acidic solutions by the bi-electron reduction of O_2 in pressed air from reaction (2-2) for the EF process.

This study focused on the effects of the electro-oxidation combined with electro-Fenton process using BDD electrodes on the degradation of biorefractory food colorant caramel. Caramel is a

representative food colorant, especially in coffee products and it is persistent and refractory to decolorize. For comparison, one of the most typical azo dyes, AO7, was used in the electrochemical decolorization of food colorants. Aqueous solutions containing Caramel Class IV, Caramel Class III and AO7 were comparatively treated by electrochemical advanced oxidation processes, including EO, EF and electro-oxidation combined with electro-Fenton (EO+EF). The experiments were performed in a stirred flask reactor using an inflator pump coupled with an undivided cell with BDD and Ti/Pt electrodes. In the EF and EO+EF process, Fe^{2+} was added as a catalyst. The independent parameters of air flow rate, Fe^{2+} concentration and current intensity in the range of 0.5-1.5 L min^{-1}, 0.05-0.2 mM and 0.4-1.5 A, respectively, were studied. The effect of electrode material on decolorization was also evaluated.

3.2 Materials and methods

3.2.1 Chemicals

Caramel Class IV, Caramel Class III and AO7 are representative colorants in food production and the Caramel Class IV and Caramel Class III are widely used in coffee products. The Caramel Class IV and Caramel Class III were supplied by Amano Foods. Applied AO7 was issued from Tokyo Chemical Industry. $FeSO_4 \cdot 7H_2O$ was used as a catalyst, as well as anhydrous Na_2SO_4 was utilized as background supporting electrolyte, they were guaranteed grade and analytical grade reagents, respectively, from Wako Pure Chemical Industries. Solutions were prepared with ultrapure water from a Direct-Q 3UV system and their pH value was adjusted to 3.0 (Brillas et al. 2009; Martínez-Huitle & Brillas 2009) with analytical grade H_2SO_4 purchased from Wako Pure Chemical Industries.

The caramel colorants showed dark color in solutions with a specific absorption wavelength of 610 nm. In the application of caramel colorants by the food industry, the yellow index was applied to analyze their quality. In regard to caramel colorants, the yellow index was measured at 470-480 nm (Qin et al., 2003).

3.2.2 Apparatus and experimental procedures

All electrolytic experiments were carried out in a 500 mL cylindrical flask reactor containing 400 ml of solution equipped with an inflator pump coupled to an undivided cell, within a water bath for maintaining the temperature of solutions at 25 °C. It was stirred with a magnetic stirrer at 800 rpm and under a given direct current condition by a DC power supply (KX-100L, Takasago Electric, Inc.). Titanium doped platinum (Ti/Pt) electrodes, with a 50 cm^2 projected area for each piece, were

supplied by Tanaka Metals Co. Ltd. Three pieces of 50 cm^2 BDD thin film from Sumitomo Electric Industries (Yoshida et al., 2007) were selected as anode and cathode, and the inter-electrode gap was 0.5 cm for each group. Experimental apparatus are illustrated in Fig. 3-1.

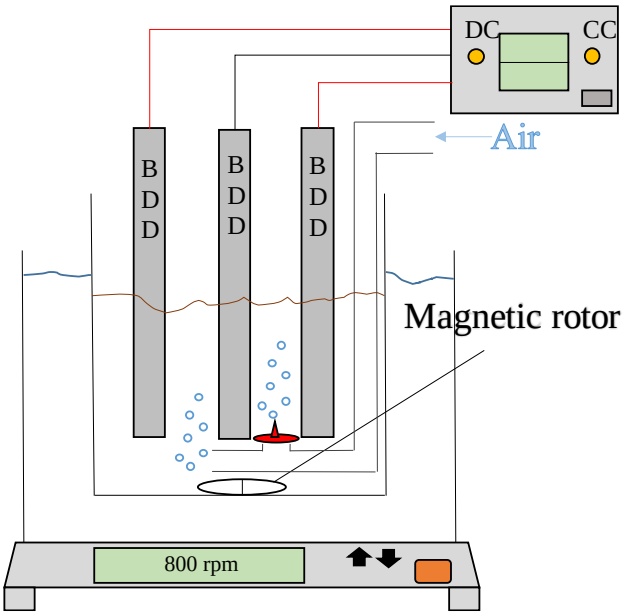

Fig. 3-1 Skeleton of experimental devices

The BDD cathodes were applied to produce H_2O_2 via reaction (2-2), which was ensured by the improvement of the air feeding system and increased rate of air flow through the solution. Prior to the experiments, a period of 30 minutes of air feeding processing was carried out with the purpose of saturating the solution with oxygen. Solutions containing 155 mg L^{-1} Caramel Class IV, 200 mg L^{-1} Caramel Class III and 25 mg L^{-1} AO7 were comparatively degraded in 0.05, 0.1 and 0.2 mM Fe^{2+}. The initial pH was adjusted to 3.0 with H_2SO_4 since this value has been found as optimal for reaction (2-1) under EF conditions.

3.2.3 Analytical methods

Each assay proceeded with decolorization from the initial solution with the same Pt-Co color unit of 5700 (dark color) to around 150 Pt-Co unit (clear state), which was the target clarity.

Every trial was performed by utilizing the solution with a selected colorant content, 0.05 M Na_2SO_4 and a given Fe^{2+} concentration in the cell, and then bubbled air at a given flow of a given rate for 30 min. Three pieces of BDD electrodes and Ti/Pt electrodes were immersed into the solution. A constant current was provided and an air pump was used to maintain the air flow through the solution to ensure O_2 feeding for the cathode. Samples were withdrawn from the solution at different times. The color removal of solutions was evaluated from their absorbance (Abs) decay at λ = 475 nm for caramel colorant and λ_{max} = 484 nm for AO7, which were determined using a UV-vis spectrophotometer (U-5100, HITACHI). The decolorization efficiency or percentage of color removal was calculated by Eq. (3-2), based on the measured absorbance at above certain wavelength (Sathishkumar et al., 2017):

$$\%\text{Color removal} = \frac{A_0 - A}{A_0} \times 100 \qquad (3\text{-}2),$$

where A_0 and A denoted the simple absorbance at the initial time and at a given time during the oxidation run, respectively. The calibration curve of the Pt-Co unit and absorbance of solutions was followed from 100 and 1000 Pt-Co unit color standard solutions (Fig. 3-2) (Cardoso et al., 2016; Sathishkumar et al. 2017). The color density of the Pt-Co value was analyzed according to the American Dye Manufactures (ADMI) Institute method (APHA Method 2120 F, 2017). The decolorization rate (R_d) was considered as an independent factor and calculated from Eq. (3-3):

$$R_d = \frac{C_0 - C_t}{C_0} \times 100\% \qquad (3\text{-}3),$$

where C_0 and C_t are the Pt-Co unit before and after the treatment, respectively.

In order to assess the energy performance of electrochemical decolorization of caramel and AO7,

the relationship (3-4) was used to calculate energy consumption (E_C) as kWh L^{-1} (Dong et al., 2021):

$$E_c = \frac{UIt}{V} \quad (3\text{-}4),$$

where U is the average voltage of the electrolyzer cell (V), I the average applied current intensity (A), t the electrolysis time (h) and V the volume of solution (L)

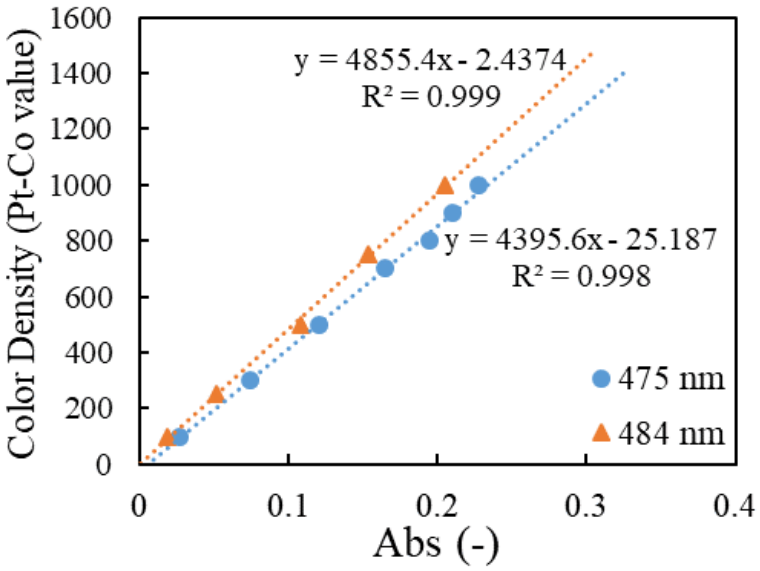

Fig. 3-2 Calibration curve of the Pt-Co value and absorbance (Abs)

3.3 Results and discussion

3.3.1 Comparative decolorization for the colorants

The comparative electrochemical trials of three different colorants were performed using the EO+EF process with BDD-BDD electrodes and 0.05 M Na_2SO_4, 0.05 and 0.2 mM Fe^{2+} solution at a pH of 3.0 and a temperature of 25 ºC. The applied air flow rate was 1.5 L min^{-1} and the current intensity was 1.5 A. In this trial, the same initial clarity in the Pt-Co unit was observed and the colorant concentration of solutions was 155, 200 and 25 mg L^{-1} for Caramel Class IV, Caramel Class III and AO7, respectively.

Figure 3-3 illustrates the effects of the variety of pigments on color absorbance (Abs) and color removal. Figure 3-3a depicts the comparison of three different colorants on decolorization with 0.05 mM Fe^{2+}, while the comparison of three different colorants on decolorization yield with 0.2 mM Fe^{2+} is shown in Fig. 3-3b. The color removal for AO7 solutions changed rapidly and further became colorless with an approximate value of 150 Pt-Co unit after 35 min, achieving 99% color decay (Fig. 3-3a). The same initial Pt-Co color unit of Caramel Class IV reached a transparent state with around 150 Pt-Co unit and 97% color removal at 154 min. The same behavior was observed for Caramel Class III, whereas the rate of color loss was slower than for Caramel Class IV, which achieved 96% color removal for 224 min oxidation time. The decolorization trends of the three colorants in Fig. 3-3b were similar to the decolorization tendency in Fig. 3-3a. Figure 3-3b shows that 96% color removal of Caramel Class IV was achieved after 189 min, while the color removal of Caramel Class III was slower and decreased by 3% in the end compared to the former trial in Fig. 3-3a.

The higher color removal rate with AO7 compared to that of Caramel could be accounted for by the fact that the colorants had a distinct chemical structure and caramel had a greater amount of

organics per unit than AO7 (Tomasik 2003; Garcia-Segura et al. 2011b). The caramel colorant was a complex mixture with separable high molecular weight and low molecular weight constituents (Tomasik, 2003), and it had a number of various chromophore and auxochromes such as carbon-carbon double bond, carbon-carbon triple bond, ketone group and amino group. Different from Caramel Class IV, Caramel Class III contains 2-Acetyl-4-tetrahydroxy-butylimidazole (THI), which was refractory and potentially toxic matter with color intensity of absorbance at 385 nm (FAO, 2011). This might contribute to the lower color removal in Caramel Class III. With regard to the AO7, on the basis of its chemical structure, it was indicated that the relative molecular weight of the AO7 was far lower than caramel and the AO7 had a single chromophore, which was an azo bond (Garcia-Segura et al., 2011b). The number, complexity, variety, and interaction of chromophore and auxochrome in colorant solution (caramel and AO7) with the same initial color unit affected the color removal rate. Fig. 3-4 presents pictures of the initial caramel solution with a Pt-Co color unit of 5700 and the treated solution with 150 Pt-Co unit. Although the AO7 solutions showed a faster performance on decolorization, the Caramel Class IV and Caramel Class III also could be decolorized completely and reached the target clarity with a clear state as shown in Fig. 3-4.

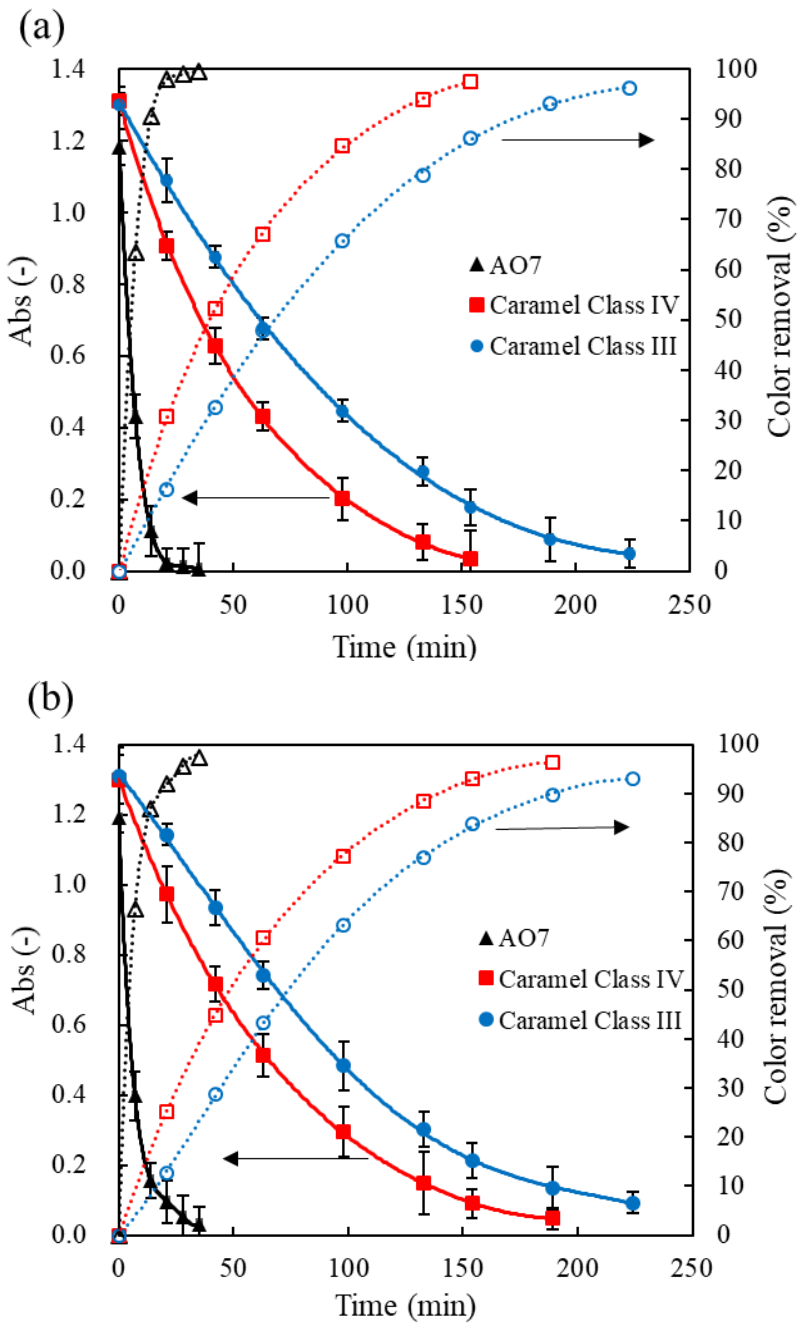

Fig. 3-3 Comparative decolorization of Caramel Class IV, Caramel Class III and AO7 by EO+EF process corresponding to absorbance (Abs) and decolorization rate (R_d) (Fe^{2+} concentration: (a) 0.05 mM, (b) 0.2 mM, Air flow rate: 1.5 L min^{-1}, Current intensity: 1.5 A, Line: absorbance, Broken line: color removal, n=3, Error bar: standard deviation)

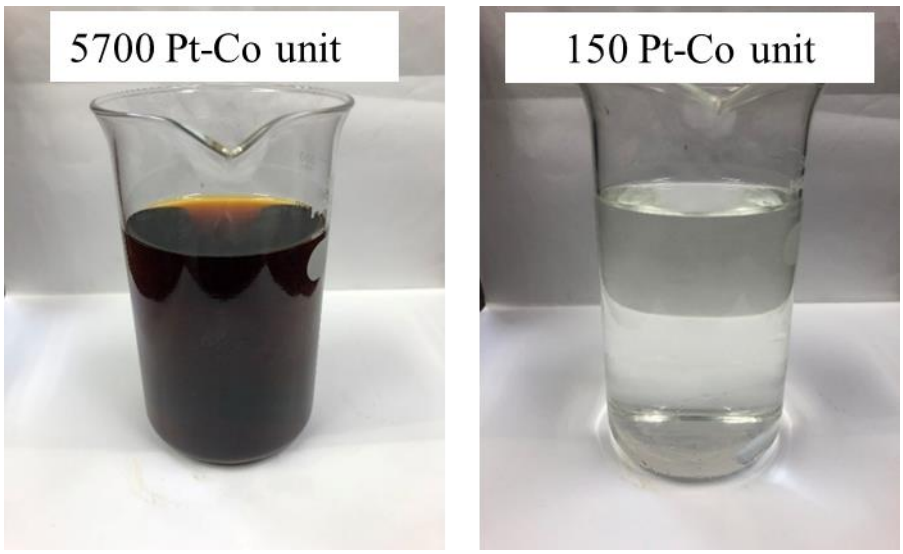

Fig. 3-4 Initial caramel solution with the color unit of a Pt-Co value of 5700 and the treated solution with a Pt-Co value of 150

3.3.2 Effect of electrode materials on decolorization

The characteristics of electrodes (anode and cathode) are key parameters assuring the efficiency of an electrochemical treatment process (Martínez-Huitle et al., 2015). It was conceivable that the EO+EF process with BDD electrodes generates ·OH and Fe^{3+} in situ by Fenton reaction (2-1) and additionally regenerated Fe^{3+} via cathodic reduction (3-5) (Özcan & Özcan, 2018), which provided an enhancement on Fenton reaction in the bulk. Based on the above observation, the combination of EO using BDD anode and EF using BDD cathode was meaningfully proposed for the efficient removal of caramel colorants.

$$Fe^{3+} + e^{-} \rightarrow Fe^{2+} \qquad (3\text{-}5)$$

The applied electrodes affected the rate of some electrochemical reactions, the rate at which BDD(·OH), H_2O_2 and Fe^{2+} were generated, and consequently the rate at which the colorants were oxidized (Martínez-Huitle et al., 2015). Fig. 3-5 showed the effect of electrode material on the decline in absorbance related to the concentration of added Fe^{2+}. The blank condition in Fig. 3-5 refers to the EO process without Fe^{2+}. The Ti/Pt anode was referred to be an active anode which indicated that the indirect oxidation predominated over direct oxidation (Kishimoto et al., 2005), while BDD was a non-active anode. Therefore a comparison between active anode and non-active anode was carried out.

Figure 3-5a depicts the decolorization performances of the EO process with Ti/Pt anode and BDD anode. The performance of decolorization applying the BDD anode was faster than the Ti/Pt anode. Fig. 3-5b illustrates that the EO process using BDD cathode reached the target clarity (Pt-Co unit) with 96% color removal at 189 min, and the EO process with Ti/Pt cathode achieved 93% color removal at 294 min. The results indicated that color removal of the EO process was affected by anode and cathode materials. The results in Fig. 3-5a confirmed that the BDD anode possessed relatively high efficiency in the decolorization of colorants. This could be attributed to the more intensive

oxidizing capacity of BDD(·OH) compared to that of ·OH generated on the Ti/Pt anode. In fact, BDD anodes had the following properties and merits: wide electrochemical window, stability under tough conditions (contaminated, organic, strong acid and strong base solutions) and relatively low background current (Yoshida et al., 2014). It was assumed that these advantages could improve the efficiency of reaction (2-1) to generate larger amounts of BDD(·OH). By comparing the two arrangements of the EO process with different cathodes in Fig. 3-5b, it corroborated that the BDD cathodes favored a higher color removal than the Ti/Pt cathode. It could be attributed to the property of the BDD cathode, which was able to produce H_2O_2 through reaction (2-2) (Yoshida et al., 2014).

The decolorization efficiency was affected by anodic and cathodic materials. Ti/Pt, classified as an active anode, merely accumulated small amounts of ·OH. In fact, these accumulated oxidants were subsequently oxidized to the weaker (less active) oxidant (MO_x), which only incurred the conversion of colorants into persistent short-chain linear carboxylic acids (El-Ghenymy et al. 2015; Duarte et al. 2018). On the other hand, BDD anode was a non-active anode, which could accumulate larger amounts of BDD(·OH). Thus, the relative oxidizing capacity of accumulated BDD(·OH) was stronger than that of accumulated ·OH generated on the Ti/Pt anode.

The decolorization assisted by the Fenton process was usually described by a first-order rate equation (Cruz-González et al., 2012). The electrochemical decolorization of Caramel Class IV with Ti/Pt and BDD electrodes exhibited first-order kinetic behavior (Eq. 3-6):

$$\ln \frac{C_0}{C_t} = k_1 t \qquad (3\text{-}6),$$

where k_1 is the apparent first-order rate constant and C_0 and C_t were the concentrations of Pt-Co color unit determined from the absorbance at the initial time and at reaction time t, respectively. The kinetic parameters determined via Eq. (3-6) were summarized in Table 3-1.

Figure 3-5c depicts the decolorization of the EO and EF process with Ti/Pt anode and BDD cathode. The process of Ti/Pt anode and BDD cathode without Fe^{2+} was the EO process, while the EF process referred to the former conditions with Fe^{2+}. A faster decolorization performance of the EF

process with 0.05 mM Fe^{2+} in solutions was observed. During the 300-min trials, the blank trial attained 30% color removal while 33% was achieved in the experiment with 0.05 mM Fe^{2+}. Fig. 3-5d shows the effects of EO and EO+EF processes on the decolorization of Caramel Class IV using BDD anode and cathode. The process applied to BDD electrodes without Fe^{2+} was the EO process, while the EO+EF process referred to the process with BDD anode and BDD cathode with Fe^{2+}. It indicated that the EO+EF process with BDD anode and cathode was more efficient on decolorization rate than the EO process under the same condition. At 154 min, the decolorization rate of the electrochemical process with different configurations of EO+EF process reached target clarity: 18.40%, 22.60%, 71.53%, 94.48% and 97.45% for EO: (Ti/Pt)-BDD, EF: (Ti/Pt)-BDD, EO: BDD-(Ti/Pt), EO: BDD-BDD and EO+EF: BDD-BDD, respectively. The similar behavior shown in Fig. 3-5 substantiated the foregoing results of the ranking of EO: (Ti/Pt)-BDD < EF: (Ti/Pt)-BDD < EO: BDD-(Ti/Pt) < EO: BDD-BDD < EO+EF: BDD-BDD. The color unit decay was analyzed from a kinetic equation related to simple reaction orders and excellent fits were obtained for a pseudo-first-order reaction (3-6), as could be seen in Table 3-1.

In the case of the EF process with Fe^{2+}, it corroborated that the EF process could accelerate decolorization more efficiently compared to the EO process, on account of a larger amount of oxidants produced by Fenton reaction (2-1) (Neyens & Baeyens, 2003). It further confirmed that the EO+EF process resulted in the highest color removal among EO, EF and EO+EF processes.

Table 3-1 Kinetic analysis assuming a pseudo-first-order reaction for Caramel Class IV and AO7

Electrochemical process	Fe^{2+} Concentration (mM)	k_1 (min^{-1})	R^2
EO: (Ti/Pt)-BDD	0	0.110×10^{-2}	0.996
EF: (Ti/Pt)-BDD	0.05	0.150×10^{-2}	0.985
EO: BDD-(Ti/Pt)	0	0.950×10^{-2}	0.994
EO: BDD-BDD	0	1.890×10^{-2}	0.993
EO+EF: BDD-BDD	0.05	2.300×10^{-2}	0.979
Fixed Conditions	Air flow rate (L min^{-1})	k_1 (min^{-1})	R^2
Caramel Class IV	1.5	2.300×10^{-2}	0.979
0.05 mM Fe^{2+}	1.0	2.010×10^{-2}	0.991
1.5 A	0.5	1.820×10^{-2}	0.983
	No air pump	1.700×10^{-2}	0.991
AO7	1.5	1.920×10^{-1}	0.994
0.05 mM Fe^{2+}	1.0	1.526×10^{-1}	0.985
1.5 A	0.5	1.247×10^{-1}	0.993
	No air pump	8.940×10^{-2}	0.998
Fixed Conditions	Fe^{2+} Concentration (mM)	k (min^{-1})	R^2
Caramel Class IV	0.2	1.760×10^{-2}	0.979
1.5 L min^{-1}	0.1	2.140×10^{-2}	0.989
1.5 A	0.05	2.300×10^{-2}	0.995
	0	1.890×10^{-2}	0.993
AO7	0.2	2.420×10^{-1}	0.996
1.5 L min^{-1}	0.1	1.932×10^{-1}	0.998
1.5 A	0.05	1.920×10^{-1}	0.994
	0	9.300×10^{-2}	0.991
Fixed conditions	Current intensity (A)	k (min^{-1})	R^2
AO7	1.5	1.920×10^{-1}	0.996
0.05 mM Fe^{2+}	0.8	1.495×10^{-1}	0.990
1.5 L min^{-1}	0.4	6.630×10^{-2}	0.995
Caramel Class IV	1.5	2.300×10^{-2}	0.979
0.05 mM Fe^{2+}	0.8	1.340×10^{-2}	0.996
1.5 L min^{-1}	0.4	1.020×10^{-2}	0.987

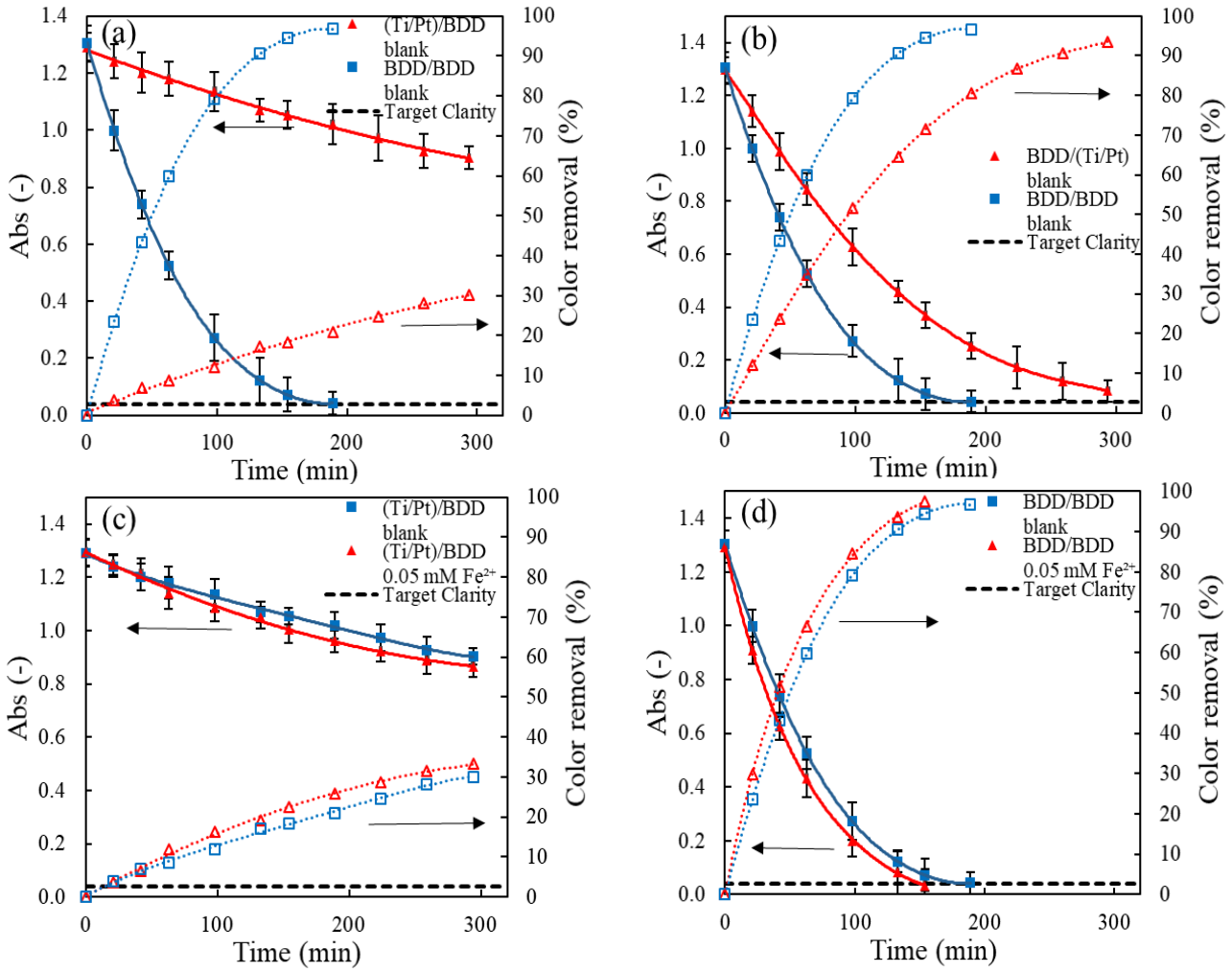

Fig. 3-5 (a) Effect of anodic material on decolorization of Caramel Class IV by EO process using BDD and Ti/Pt anode; (b) Effect of cathodic material on decolorization of Caramel Class IV by EO process using BDD cathode and Ti/Pt cathode; Effect of EO, EF and EO+EF process on decolorization of Caramel Class IV using (c) Ti/Pt anode and BDD cathode, (d) BDD anode and BDD cathode (Fe^{2+} concentration: 0 and 0.05 mM, Air flow rate: 1.5 L min^{-1}, Current intensity: 1.5 A, Line: absorbance, Broken line: color removal, n=3, Error bar: standard deviation)

3.3.3 Effect of air flow rate on decolorization

The air flow rate on the EF process was a key parameter for cathodic reaction as it is related to the generation of H_2O_2. The effect of air flow rate on the degradation of 25 mg L^{-1} AO7 and 155 mg L^{-1} Caramel Class IV solution with 0.05 mM Fe^{2+} at 1.5 A constant current by EO+EF with BDD electrodes process was investigated between 0.5 L min^{-1} and 1.5 L min^{-1} air flow rate (Fig. 3-6).

Figure 3-6a highlights that the solution with caramel became colorless at a shorter time with increasing air flow rate, from 0.5 to 1.5 L min^{-1}. At the end of the electrolyte process, the color removals were achieved from 95 % for a blank condition to 97 % for 1.5 L min^{-1}. In Fig. 3-6a, the EO+EF process without air feeding yielded the slowest decolorization and reached the target clarity at 190 min. However, as for the EO+EF process with an airflow rate of 1.5 L min^{-1}, the color removal reached the target clarity in 155 min. The pseudo-first-order reaction was used to simulate the decolorization process by electro-oxidation treatment (Eq. 3-7) (Garcia-Segura et al. 2011b; Thiam et al. 2015):

$$A = A_0 \cdot e^{-kt} \qquad (3\text{-}7),$$

where A_0 and A were the absorbance at the initial time and time t at the corresponding wavelength, respectively. k was determined as the slope of the linear fitting between absorbance decay and t.

The results in Table 3-1 showed a gradual increase in k value with air flow rate, which suggested that the progressive acceleration of cathodic reactions generated larger amounts of H_2O_2 through reaction (2-2) due to the increase of dissolved oxygen in solutions, and consequently, enhanced the rate of Fenton reaction (2-1).

A similar trend of Fig. 3-6a could be observed in Fig. 3-6b where higher color removal was achieved from 97% for blank trial to 99% for 1.5 L min^{-1}. It was noticed in Fig. 3-6b that the absorbance values declined sharply with the air feeding system regardless of air flow rate value, while the values dropped smoothly without air feeding with a longer reaction time of 42 min. These results

indicated that increasing air flow rate enhanced the decolorization of Caramel Class IV and AO7, owing to the acceleration of electro-Fenton reactions.

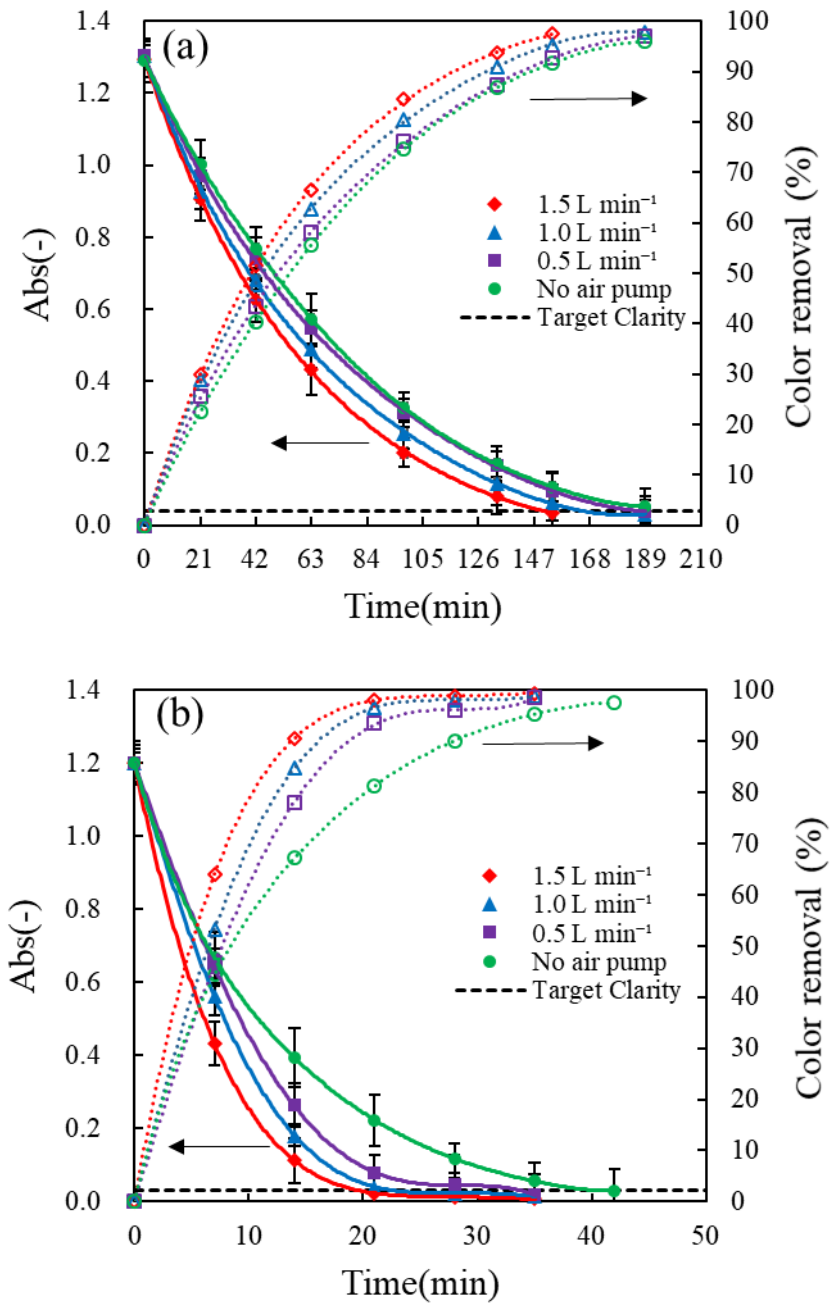

Fig. 3-6 Effect of air flow rate on decolorization of (a) Caramel Class IV and (b) AO7 by EO+EF process (Fe^{2+} concentration: 0.05 mM, current intensity: 1.5 A, Line: absorbance, Broken line: color removal, n=3, Error bar: standard deviation)

3.3.4 Effect of ferrous ion concentration on decolorization

The hydroxyl radicals were generated from the Fenton reagent, and the Fe^{2+} concentration was involved in the hydroxyl radical generation, according to reaction (2-1). To gain insight into the decolorization yield of caramel colorant and AO7, the effects of Fe^{2+} concentration on the decolorized performances of EO and EO+EF using BDD-BDD cells were investigated. AO7 and Caramel Class IV solutions with the same initial Pt-Co color unit and 1.5 L min^{-1} flow rate were electrolyzed between 0 and 0.2 mM Fe^{2+} under 1.5 A current intensity.

Figure 3-7 illustrates the results obtained with caramel and AO7 solutions when the catalyst content varied between 0 and 0.2 mM. Fig. 3-7a depicts that when the catalyst content was above 0.1 mM, the color rate decreased and even was similar to that without Fe^{2+}. However, different results were obtained with the AO7 decolorization yield. Fig. 3-7b shows that AO7 established a positive correlation with Fe^{2+} concentration and absorbance abatement, required 42 min at 0 mM Fe^{2+} and 21 min at 0.05, 0.1, 0.2 mM Fe^{2+}, to reach at least 97% color removal. This tendency could be corroborated by the pseudo-first-order kinetic analysis of two colorants presented in Table 3-1. With regard to AO7, a rise in *k*-value was found at a higher Fe^{2+} concentration, being 2.6-fold, 2.08-fold and 2.06-fold higher at 0.2, 0.1 and 0.05 mM, respectively, as compared with without Fe^{2+}. In contrast, as for the caramel colorant, no further enhancement was achieved beyond 0.05 mM Fe^{2+} concentration.

The results from Fig. 3-7 could be explained by progressive upgrades of ·OH generation from the Fenton reaction (2-1) as a result of the increase of Fe^{2+} concentration. On the contrary, the excess of catalyst could lead to efficiency decline because it eliminates partial ·OH as shown in reaction (3-8) (Sirés et al., 2014).

$$Fe^{2+} + \cdot OH \rightarrow Fe^{3+} + OH^{-} \qquad (3\text{-}8)$$

For caramel, it could be concluded that within a given scale, increasing Fe^{2+} concentration could promote the Fenton reaction (2-1), whereas higher Fe^{2+} and/or generated ·OH could react with each

other and consume themselves via reaction (3-8). Moreover, the Fe^{3+} complexes, a colored matter (El-Ghenymy et al. 2015; Thiam et al. 2015), generated during electrolyte. They imposed an interference on absorbance as they had a certain absorbance which corresponded to a constant Pt-Co unit around 475 nm.

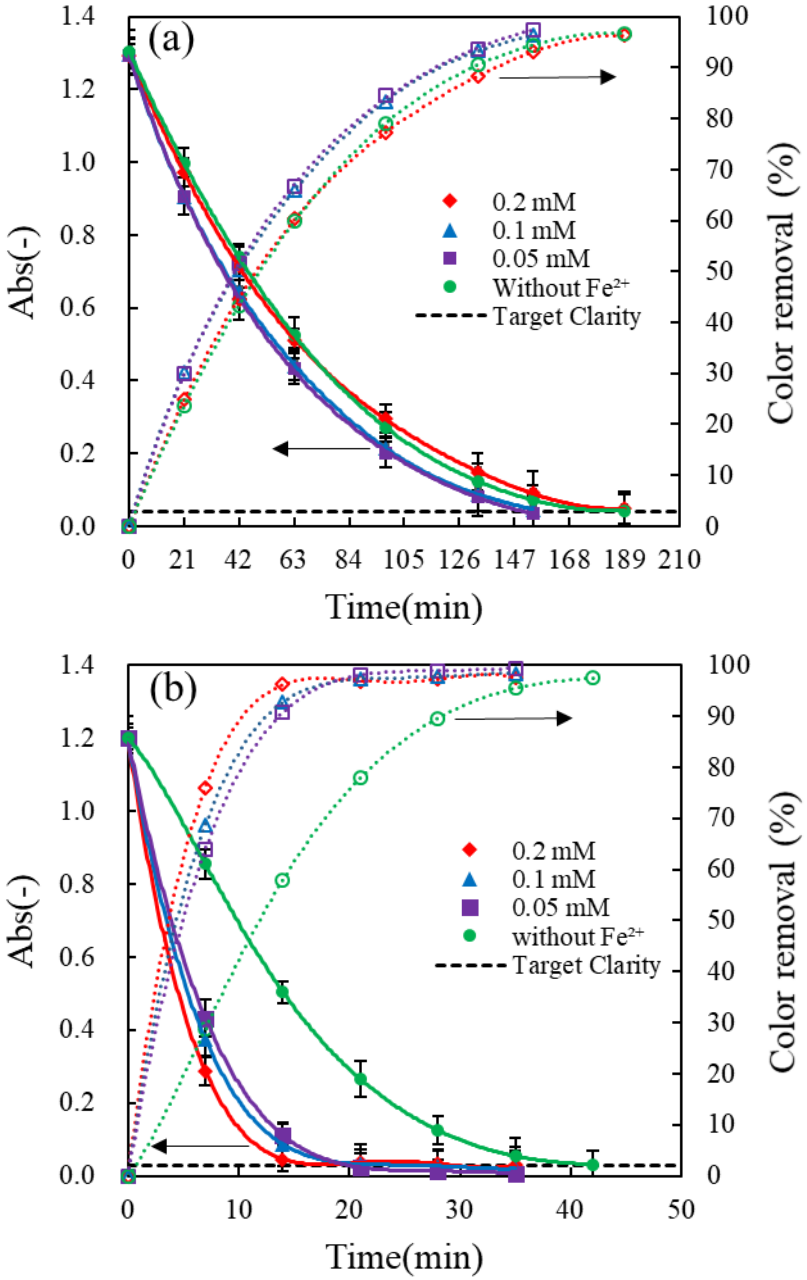

Fig. 3-7 Effect of Fe^{2+} concentration on decolorization of (a) Caramel Class IV and (b) AO7 by EO+EF process or EO process (air flow rate: 1.5 L min^{-1}, current intensity: 1.5 A, Line: absorbance, Broken line: color removal, n=3, Error bar: standard deviation)

3.3.5 Effect of current intensity on decolorization

The applied current was the driving force for both the oxygen reduction, which gave rise to hydrogen peroxide generation at the cathode, and the production of physisorbed BDD(·OH) on the surface of the anode (Ou et al., 2020). The effects of current intensity on the decolorization of 25 mg L^{-1} AO7 and 155 mg L^{-1} Caramel Class IV solutions with 0.05 mM Fe^{2+} applying 1.5 L min^{-1} air flow rate by EO+EF-BDD process was investigated between 0.4 A and 1.5 A.

The changes in decolorization rate with prolonging time for the EF process at three different current intensity values were investigated and the results are shown in Table 3-1. The changes in AO7 in Fig. 3-8 indicate almost the same decolorization curve and charge utilization between 0.8 and 0.4 A current intensity conditions. Under the 1.5 A current intensity condition, the charge utilization of the decolorization curve was lower than the 0.8 and 0.4 A conditions. With respect to the caramel solution, more obvious trends of increasing current intensity causing a loss of the charge utilization (charge utilization: 1.5 A < 0.8 A < 0.4 A) are shown in Fig. 3-8. It was assumed that higher current intensity resulted in a higher amount of BDD(·OH) generated by anodic reaction as well as of H_2O_2 yielded at the cathode via reaction (2-2), which favored the larger generation of (·OH) from Fenton reaction (2-1). However, the decrease in the charge utilization with the increase of current intensity could be explained from two aspects. One aspect was caused by the enhancement of competitive electrode reactions. The discharge of oxygen at the anode and evolution of hydrogen at the cathode occurred at higher current intensity (Nidheesh & Gandhimathi, 2012). Moreover, the BDD(·OH) production could be inhibited by the generation of other weaker oxidants such as $S_2O_8^{2-}$ via reaction (3-9) (Panizza & Cerisola, 2009). These side electrode reactions inhibited the main reactions (2-2), (3-5) and anodic reactions, which resulted in a decrease in charge utilization. The other aspect could refer to the consumption of excess yielded (·OH), which is caused by a non-oxidizing parasitic reaction (Ltaïef et al., 2018). These side reactions could incur the removal of (·OH) by reaction (3-8)

and the loss of H_2O_2 through reaction (3-10) (Zhang et al., 2007).

$$2SO_4^{2-} \rightarrow S_2O_8^{2-} + 2e^- \quad (3\text{-}9)$$

$$H_2O_2 + \cdot OH \rightarrow HO_2 \cdot + H_2O \quad (3\text{-}10)$$

The proportion between expenses and the outcome of electrolysis should be well considered. The energy consumption was calculated by equation (3-4). The energy consumption of the EO+EF process (0.05 mM Fe^{2+}) and EO process (without Fe^{2+}) were 12.77 kWh L^{-1} and 16.05 kWh L^{-1}, respectively, for AO7 decolorization under conditions of 1.5 A, 1.5L min^{-1}, BDD-BDD. With respect to caramel VI, the energy consumption of the EO+EF process (0.05 mM Fe^{2+}) and EO process (without Fe^{2+}) were 53.43 kWh L^{-1} and 67.15 kWh L^{-1} at 1.5 A, 1.5 L min^{-1} flow rate with BDD-BDD electrode. The combination of the EO+EF process could save more energy than the EO process whether for decolorization of AO7 or caramel VI colorants.

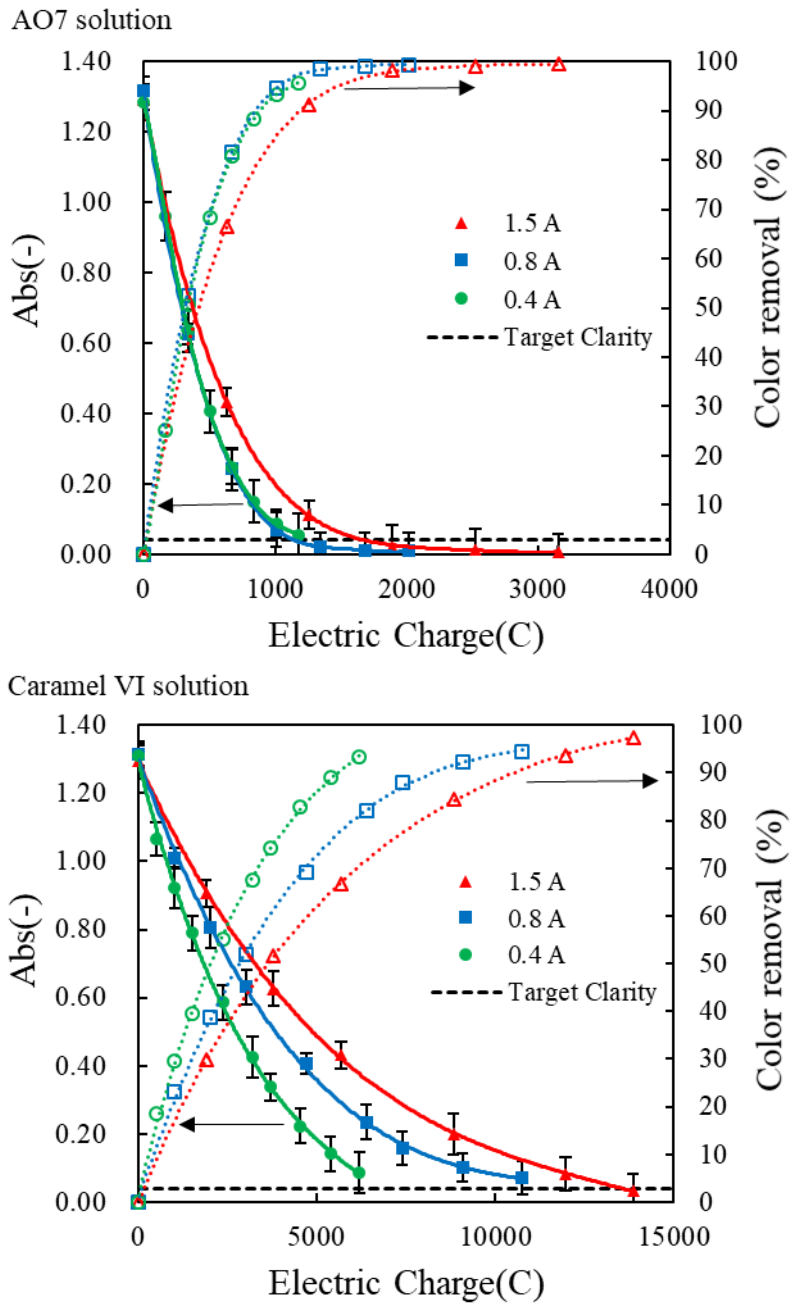

Fig. 3-8 Effect of current intensity on electric charge consumption of Caramel Class IV and AO7 by EO+EF process (Fe^{2+} concentration: 0.05 mM, air flow rate: 1.5 L min^{-1}, Line: absorbance, Broken line: color removal, n=3, Error bar: standard deviation)

3.4 Conclusion

The decolorization rate of Caramel Class IV was investigated by EO, EF and EO+EF process with BDD and Ti/Pt electrodes. The caramel was decolorized almost completely with the shortest electrolyte time (154 min) by the EO+EF process using BDD electrodes with the addition of 0.05 mM Fe^{2+}, via applying 1.5 L min^{-1} air flow rate and 1.5 A current intensity. The decolorization of AO7 exceeded 99% within 40 min under all experimental conditions. It suggested that the caramel was more difficult to degrade than AO7 owing to its complicated constituents. However, a complete decolorization of caramel (lower 150 Pt-Co unit) was still observed under the experimental condition, and the highest kinetic constant of 2.3×10^{-2} min^{-1} was found under these conditions. The results of the effect of electrode material indicated that the performances of EO, EF and EO+EF processes, were affected by the anode and cathode materials. Especially, BDD anode and cathode favored better decolorization yield than other electrode materials. The decolorization efficiency has been investigated and listed in increasing order as follows: EO: (Ti/Pt)-BDD < EF: (Ti/Pt)-BDD < EO: BDD-(Ti/Pt) < EO: BDD-BDD < EO+EF: BDD-BDD. A higher concentration of Fe^{2+} caused a faster discoloration, meanwhile, it could lead to the removal of Fe^{2+} and ·OH, as well as some interferences on account of its oxidized complex. The color loss always obeyed a pseudo-first-order kinetics and the reaction rate *k* varied positively and linearly with the air flow rate and current intensity. Higher current intensity accelerated the color removal. However, it was detrimental to the electric charge consumption due to the parasitic reaction. The EO combined with the EF process using BDD electrodes was an effective treatment for color removal of caramel colorants, allowing a significant decolorization to be achieved.

Chapter Four

Electrochemical decolorization of liquid digestate from anaerobic digestion of coffee waste using the boron-doped diamond (BDD)

This paper was accepted by the International Journal of Environmental Science and Technology

4.1 Introduction

High turbidity in digestate hinders the permeation of light into the medium and is a major issue for the use of digestate in microalgae cultivation (Monlau et al., 2015). EO has been widely applied for the decolorization of wastewater containing methyl orange (Wang et al., 2020) and malachite green (El-Ghenymy et al., 2015). The EO process can decompose complex refractory contaminations into small biodegradable molecules and greatly improve the biodegradability of wastewater (Krzemińska et al., 2015). In decolorization by EO, electrochemically generated hypochlorite has been used from chloride ions in the solution (Martínez-Huitle et al., 2015). This production of hypochlorite by the electrochemical reaction reduces the concentration of NH_4-N, which is a nutrient source for algae. The selection of an appropriate anode material is important for the EO process. As an electrode, BDD provides a high overpotential for oxygen production and a wide potential window. Because of these properties, rather than generating and using hypochlorite, BDD anodes generate ·OH and use it to oxidize organic compounds (Panizza & Cerisola, 2005).

Coffee waste biomass is a potential substrate for anaerobic digestion, whereas it also remains dark color such as the caramel. Therefore the electrochemical decolorization which is especially effective on the refractory caramel is necessary for producing a highly light-permeable medium. The objective of this study was to evaluate the decolorization of anaerobic digestate from spent coffee

grounds (SCG) using a BDD anode for EO. The decolorization performance and NH_4-N concentration in the anaerobic digestate were investigated. An anaerobic liquid digestate from coffee waste biomass and another kind of typical digestate from dairy cow manure were compared to investigate their decolorization properties. This study compared the SCG digestate with cow manure (CM) digestate to evaluate the effect of the substrate on anaerobic digestion. The effects of the anodic material, initial Fe^{2+} concentration, and current on the EO process were also investigated. To evaluate the performance, the color removal rate, absorbance decay, COD removal, and changes in the NH_4-N concentration were analyzed.

4.2 Materials and methods

4.2.1 Chemicals

The catalyst ($FeSO_4 \cdot 7H_2O$, guaranteed grade reagent) was purchased from FUJIFILM Wako Pure Chemical Corporation (Osaka, Japan) and used in the experiments at 0.1, 0.2, 0.4, 0.8 mM. Solutions were prepared with deionized water, which was produced by a Direct-Q 3UV system.

4.2.2 Digestate

Two types of digestates were used in this study. The CM digestate was obtained from a small-scale anaerobic digester fed with dairy CM at a dairy farm in Kansai, Japan. The SCG digestate was collected from a laboratory-scale anaerobic reactor fed with simulated coffee waste. The simulated coffee waste was prepared from coffee powder (Golden Special Coffee, UCC, Japan). First, the coffee powder was fully dissolved in 100 mL of distilled water at 70 °C to prepare a coffee solution. Then, the coffee solution was filtered through coffee filter paper (20 μm) to obtain filtered coffee waste as a substrate. The inoculum for anaerobic digestion of the simulated coffee waste was obtained from a biogas plant at a food processing facility in Kansai, Japan. The characteristics of the SCG digestate are shown in Table 4-1.

4.2.3 Apparatus and experimental procedures

Each digestion reactor had a working volume of 700 mL and a total volume of 1000 mL. After the inoculum was added to the reactor, the reactor was placed in an incubator at 37 °C for 72 h before the addition of the substrate. The inoculum and substrate were mixed in the reactor by manual shaking. Anaerobic digestion was performed with 30% headspace under a N_2 atmosphere, and the vials were sealed with a butyl cap and plastic thread. The biogas is collected in a composite aluminum bag throughout the anaerobic digestion process.

After anaerobic digestion, the digestate was obtained by filtering the reaction mixture through a mesh filter and remaining the filtrate. The digestate then was centrifuged twice (4347 ×*g*, 15 min) to separate the SS and solution. Liquid digestate was obtained by membrane filtration (0.2 μm, MICRODYN, Germany) of the solution.

For EO, the liquid digestate was diluted two-fold. The anode for the EO was BDD (Sumitomo Electric Industries), platinum-doped titanium mesh sheet (Ti/Pt, Tanaka Kikinzoku Kogyo Co., Ltd), or IrO_2 doped titanium mesh (Ti/IrO_2, Tanaka Kikinzoku Kogyo Co., Ltd), and the cathode was BDD (Sumitomo Electric Industries). The EO experiments were carried out in a 500-mL flask reactor with 400 mL of solution. A water bath was used to maintain the temperature of the solutions at 35 °C. The reaction mixtures were stirred with a magnetic stirrer at 800 rpm and under constant current conditions at 0.6, 0.9, 1.2, 1.5, or 2.0 A (KX-100L DC power supply, Takasago Electric). The inter-electrode gap was 0.5 cm and the immersed area of each electrode was 35 cm^2. The flow diagram of the experimental procedure is shown in Fig. 4-1.

Table 4-1 Characteristics of the SCG digestate

Parameters	Concentrations and values
COD (mg L^{-1})	7600 ± 640
NH_4-N (mg L^{-1})	1520 ± 240
NO_2-N (mg L^{-1})	39 ± 11
TN (mg L^{-1})	1762 ± 76
TOC (mg L^{-1})	1142 ± 285
TSS (mg L^{-1})	340 ± 80
PO_4-P (mg L^{-1})	212 ± 48
Cl^- (mg L^{-1})	792 ± 40
Na^+ (mg L^{-1})	252 ± 60
K^+ (mg L^{-1})	524 ± 37
Color (Pt-Co value)	11000 ± 850
pH	6.1 ± 0.5

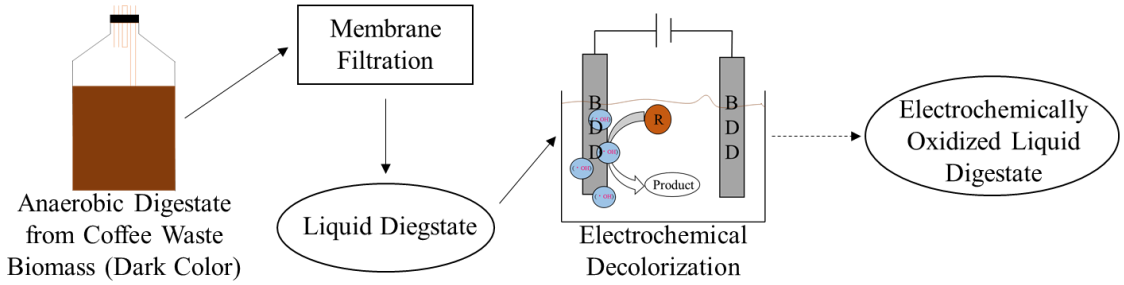

Fig. 4-1 Flow diagram of the experimental procedure

4.2.4 Analytical methods

The absorbance values of the solutions were measured by ultraviolet–visible spectrophotometry (U-5100, HITACHI, Japan). A calibration curve for the platinum-cobalt (Pt-Co) color scale against the absorbance was constructed using color standard solutions with Pt-Co values of 100 and 1000 (Cardoso et al., 2016; Sathishkumar et al., 2017). The color removal was calculated from the absorbance measured at 475 nm and the calibrated Pt-Co value as follows:

$$\text{Color removal} = \frac{C_0 - C_t}{C_0} \times 100\% \qquad (4\text{-}1),$$

where C_0 and C_t denoted the Pt-Co value and that at time t during the EO, respectively.

All parameters were analyzed according to the Standard Method for Examination of Water and Wastewater (APHA, 2017). The COD and the concentration of PO_4^{3-} were measured using a spectrometer (DR3900, HACH, USA). To determine the contents of NH_4^+, Na^+, K^+, Cl^-, NO_2^-, and PO_4^{3-}, the raw SCG digestate was analyzed by ion chromatography (IC-8100, TOSOH, Japan). The total nitrogen (TN) and total organic carbon (TOC) were measured by a TN and TOC analyzer (TNM-L, TOC-L, Shimadzu, Japan). The color density was analyzed according to the American Dye Manufactures Institute (ADMI) method (APHA Method 2120 F, 2017). A target was established as the absorbance at 475 nm of a clear and colorless solution with a Pt-Co value of 200.

4.3 Results and discussion

4.3.1 Electrochemical oxidation of CM digestate and SCG digestate

The CM and SCG digestates were treated by EO using a Ti/Pt anode and BDD cathode with a current of 1.5 A. Both digestates had a similar initial absorbance at 475 nm. Figure 4-2 shows the change in the absorbance and color removal for the different digestates. The dashed line shows the target value for the absorbance at 475 nm of a clear and transparent solution with a Pt-Co value of 200. The color of the CM digestate changed rapidly and the solution became colorless and nearly clear after 720 min with an absorbance value close to the target (Fig. 4-2a). The color removal rate was 97.6% (Fig. 4-2b). For the SCG digestate, the absorbance at 475 nm decreased to reach the target value at 810 min (Fig. 4-2a), and the color removal rate was 97.8% (Fig. 4-2b). The higher color removal rate of the CM digestate compared with that of the SCG digestate could be attributed to the following. First, a high concentration of chlorine in the CM digestate might enhance the EO process via indirect oxidation. Second, the substrate for SCG digestion was roasted coffee beans, which meant that the SCG digestate contained caramel and melanoidin in addition to humus-like and fulvic acid-like colored matter (Monlau et al., 2015). Caramel is a complex mixture that contains high and low molecular weight compounds (Tomasik, 2003) and is rich in auxochromes and chromophores that contain carbon-carbon covalent bonds, amino groups, ketone groups. Melanoidins are high molecular weight compounds with a dark brown color (Moreira et al., 2012). The contents of caramel and melanoidin in the SCG digestate would increase its decolorization time compared with the CM digestate.

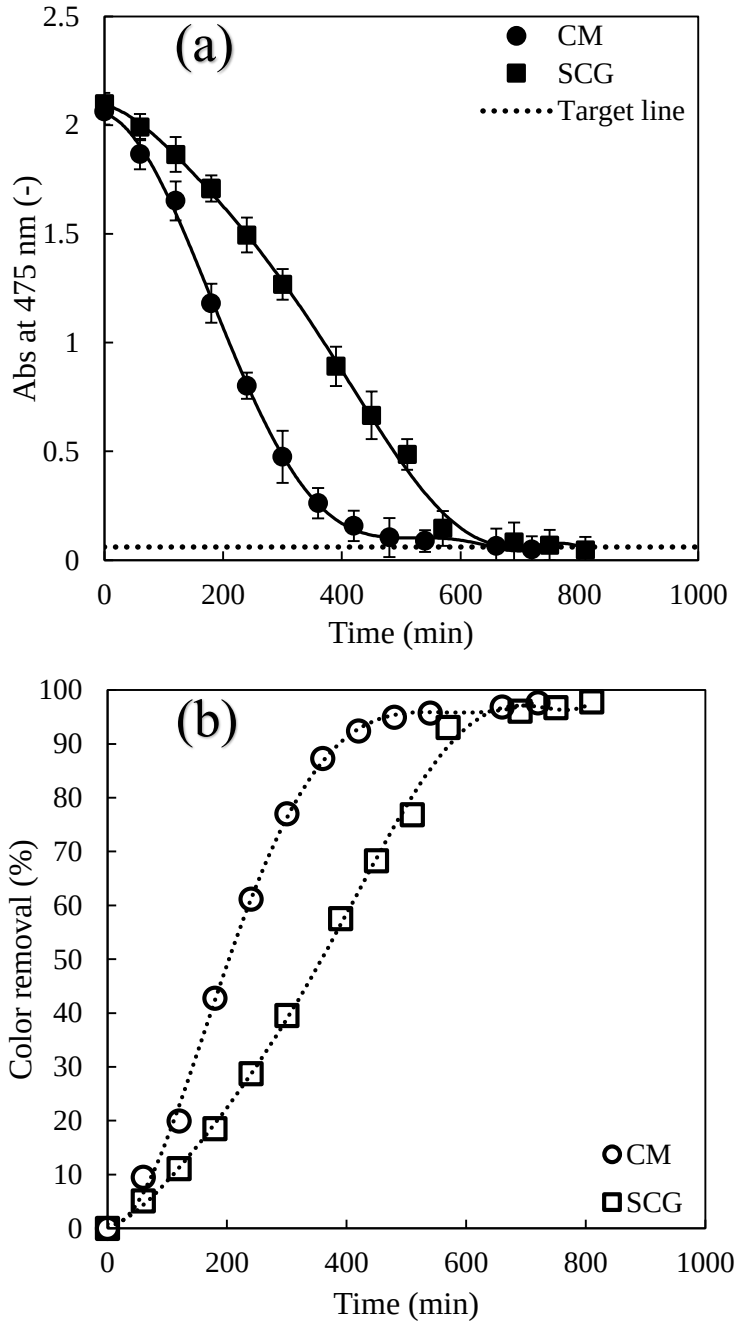

Fig. 4-2 (a) Absorbance and (b) color removal rate over time for the electrochemical decolorization of SCG and CM digestates with a Ti/Pt anode and a BDD cathode (current intensity 1.5 A, no addition of Fe^{2+} concentration, n=3, Error bar: standard deviation)

4.3.2 Effect of the anode material on decolorization of the SCG digestate

The anode properties are important for efficient EO. The anode affects the rate of an electrochemical reaction, including the generation of oxidants, and consequently affects the oxidation of colorants (Martínez-Huitle et al., 2015).

Figure 4-3 shows the effect of the anode material on the absorbance of the SCG digestate. The dashed line shows the target value for the absorbance at 475 nm of a clear and transparent solution with a Pt-Co value of 200. The decolorization with the BDD anode was much more rapid than with the Ti/Pt or Ti/IrO_2 anode. With the BDD anode, the target color (Pt-Co value of 200) and 98.7% color removal were reached at 270 min. By contrast, with the Ti/Pt anode, it took 720 min for the decolorization to reach the target and the color removal was only 97.5%. With the Ti/IrO_2 anode, the decolorization required even more time (1020 min) and the color removal rate was lower (97.1%). These results were attributed to the nature of the inactive BDD anode, which has a wide electrochemical window and produces large quantities of ·OH radicals and other active species on its surface. According to previous research (Fernandes et al., 2015), the generated ·OH is weakly physisorbed on the BDD anode and facilitates the oxidation of organic compounds. By contrast, ·OH is strongly chemisorbed on the active anodes of Ti/IrO_2 and Ti/Pt, and the oxidation of organic compounds with these anodes is inferior to that of BDD (Mandal et al., 2017). Furthermore, the concentration of chlorine in the SCG digestate was low, which resulted in weak indirect oxidation by the Ti/Pt and Ti/IrO_2 anodes. The comparison of the three anodes showed that the anode material greatly affected color removal in EO and that the BDD anode was best for decolorization.

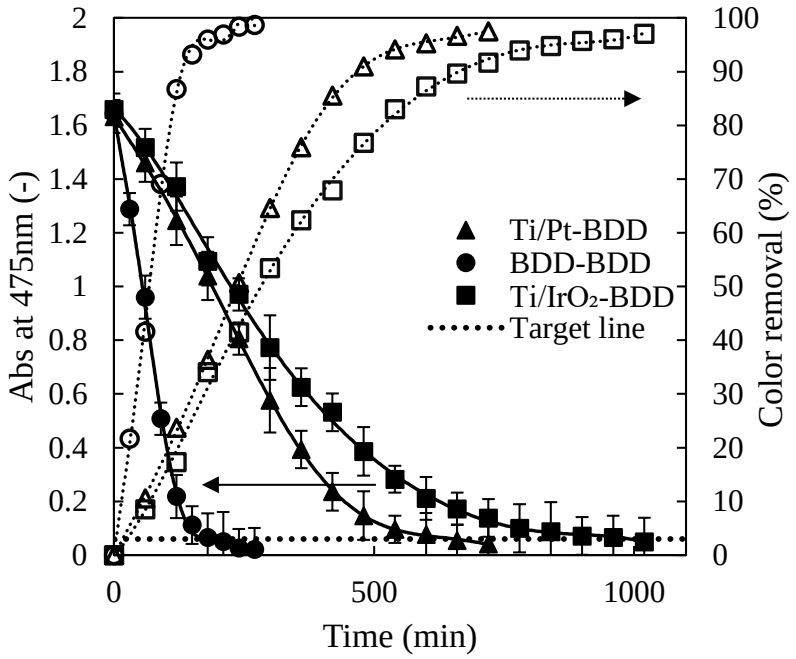

Fig. 4-3 Effect of anode material (BDD, Ti/Pt, or Ti/IrO_2) on the decolorization (absorbance and color removal) of SCG digestate (BDD cathode, current intensity 1.5 A, no addition of Fe^{2+} content, Line: absorbance, Broken line: color removal, n=3, Error bar: standard deviation)

4.3.3 Effect of the ferrous ion concentration on degradation of the SCG digestate

Fenton's reagent, which contains Fe^{2+} and H_2O_2, can generate hydroxyl radicals by Fenton's reaction. Therefore, the Fe^{2+} concentration in EO is important for the generation of hydroxyl radicals. In this study, the effect of Fe^{2+} concentration (0–0.8 mM) was investigated using SCG digestate solutions with the same initial absorbance at 475 nm and EO at 1.5 A.

Figure 4-4 shows the change in absorbance for the SCG digestate. The dashed line shows the target value for the absorbance at 475 nm of a clear and transparent solution with a Pt-Co value of 200. Up to 100 min, the decolorization increased with increases in the Fe^{2+} concentration. Up to 270 min, the change in color removal was not greatly associated with an increase in initial Fe^{2+} concentration (Fig. 4-4 and Table 4-2). The effect on the absorbance could be attributed to the fact that Fenton's reaction produced a larger amount of ·OH as the Fe^{2+} concentration increased. However, an excess of Fe^{2+} might have adverse effects on oxidation because some ·OH would be consumed as shown in reaction (4-2) (Sirés et al., 2014).

$$Fe^{2+} + \cdot OH \rightarrow Fe^{3+} + OH^{-} \qquad (4\text{-}2)$$

Colored complexes of Fe^{3+} and Fe^{2+} (Thiam et al., 2015) might be produced as by-products of the EO, and these complexes will affect the absorbance at 475 nm and the Pt-Co value.

Changes in the concentration of Fe^{2+} also affected the COD removal. Up to 270 min, the COD removal increased with increases in the Fe^{2+} concentration (Table 4-2). COD removal rates of 84.2%, 85.5%, 87.1%, and 89.2% were obtained with 0.1, 0.2, 0.4, and 0.8 mM Fe^{2+}, respectively. The improvement in COD removal up to 270 min with increases in the initial Fe^{2+} concentration contrasted with the results for color removal, where improvements were only observed up to 100 min (Fig. 4-4 and Table 4-2). This difference in the results is consistent with the effect of Fe^{2+} on the formation of colored complexes (Ertugay & Acar, 2017).

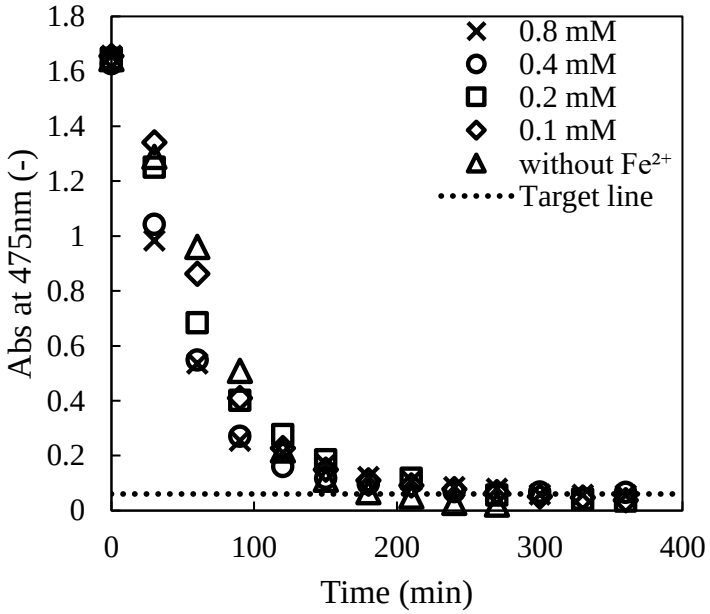

Fig. 4-4 Effect of the Fe^{2+} concentration on the absorbance for the SCG digestate treated with a BDD anode and BDD cathode (current intensity 1.5 A, initial additional Fe^{2+} of 0.1 to 0.8 mM)

Table 4-2 Effects of added Fe^{2+} on the color removal rate and chemical oxygen COD removal for SCG digestate treated with a BDD anode (270 min)

Initial additional Fe^{2+} concentration (mM)	Color removal (%)	COD removal (%)
0	98.7	84.1
0.1	97.0	84.2
0.2	96.7	85.5
0.4	95.9	87.1
0.8	95.2	89.2

4.3.4 Effect of the current on decolorization of the SCG digestate

The current is a key parameter that affects generation of hydrogen peroxide via cathodic oxygen reduction and generation of physisorbed ·OH on the BDD anode surface (Ou et al., 2020). The effect of the current (0.6–2.0 A) on the decolorization of SCG digestate by the EO process was investigated.

The relationship between the absorbance decay and electric charge for the EO process is shown in Fig. 4-5. With a current of 1.5 A, the absorbance decreased faster than with a current of 0.6, 0.9, 1.2, or 2.0 A (Fig. 4-5a). The above results were validated by a pseudo-first-order kinetic analysis of the SCG digestate decolorization (Fig. 4-5b). The pseudo-first-order reaction was applied to model the electrochemical decolorization process (Eq. 4-3) (Garcia-Segura et al., 2011; Thiam et al., 2015) as follows:

$$A = A_0 \cdot \mathrm{e}^{-kEC} \qquad (4\text{-}3),$$

where A_0 and A are the absorbance at 475 nm with the initial electric charge and a given electric charge (EC), respectively. The k was determined as the slope of the linear regression line between the relative absorbance ($\ln A_0/A$) and EC. The kinetics analysis is shown in Fig. 4-5b. A positive relationship was established between the current (0.6–1.5 A) and absorbance decay. With a current of 2.0 A, the absorbance decay was the slowest. The results in Fig. 4-5a and Fig. 4-5b could be explained by an increase in competitive electrode reactions, including side reactions and parasitic reactions. Moreover, a higher current would enhance oxygen evolution at the anode and hydrogen evolution at the cathode (Nidheesh & Gandhimathi, 2012).

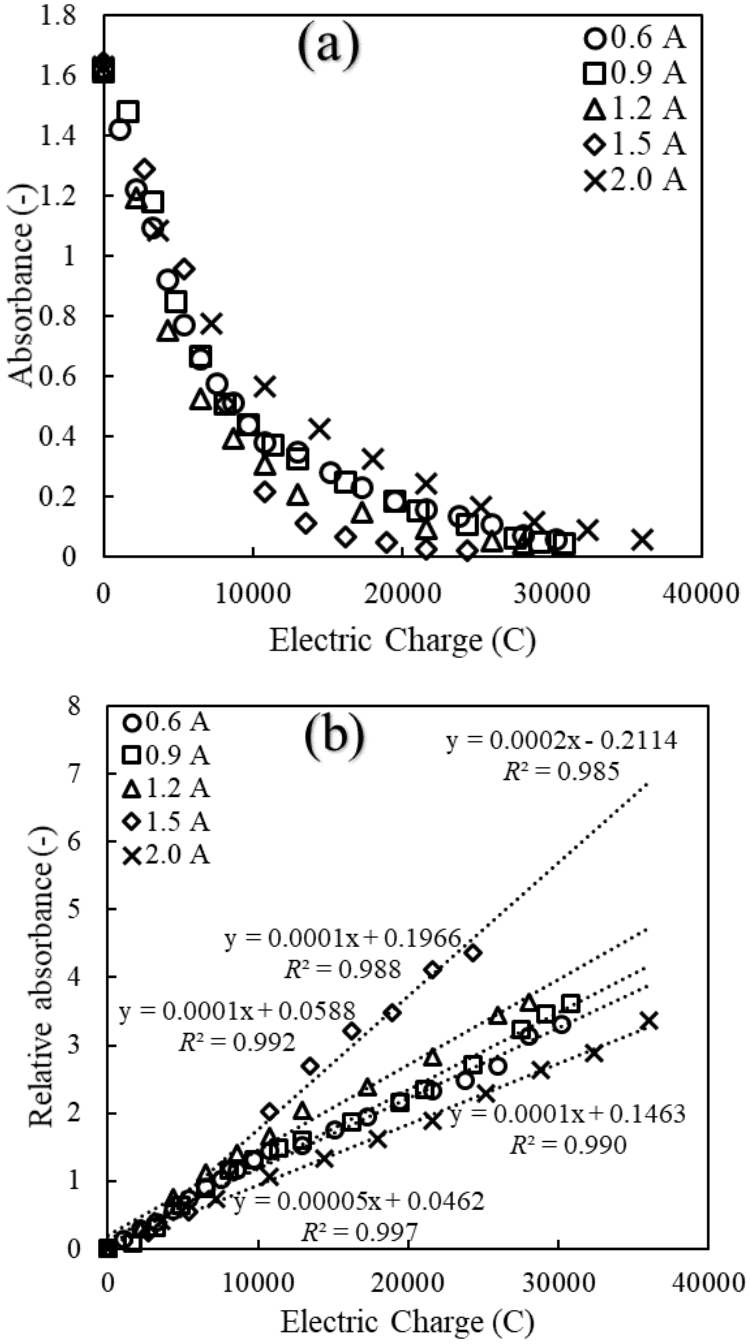

Fig. 4-5 Effect of the current on (a) the absorbance and (b) the relative absorbance for decolorization of the SCG digestate (BDD anode, BDD cathode, current intensity: 0.6 to 2.0 A, no addition of Fe^{2+})

4.3.5 Changes in the nutrients in the SCG digestate during the EO process

Ammonium and phosphate in digestate can be used in microalgae cultivation (Sayedin et al., 2020; Pulgarin et al., 2021). In the present study, changes in the NH_4-N, COD, and color during membrane filtration pre-treatment and EO were investigated.

Membrane filtration reduced the NH_4-N by 27.4%, the COD by 42.1%, and the Pt-Co value by 32% (Fig. 4-6). The reduction in NH_4-N was attributed to the pore size of membrane used for filtration. The high COD removal by the membrane indicated that some organic compounds in the digestate were in the form of suspended particles (> 1.2 μm) (Akhiar et al., 2017) and other macromolecular substances that were larger than the pore size of membrane (0.2 μm). These organic particles would be retained on the membrane, and this would also trap any ammonium ions that were absorbed on the particles. Most of the reduction in the Pt-Co color value was attributed to SS, which was removed by the membrane.

Figure 4-7 shows the changes in NH_4-N and COD removal during EO with BDD and Ti/Pt anodes. In each case, the absorbance of the treated solution at 475 nm reached the target (Pt-Co value of 200). The NH_4-N concentration decreased by 12.6% with the BDD anode and 22.7% with the Ti/Pt anode (Fig. 4-7a). For the COD, the BDD and Ti/Pt anodes showed large differences (Fig. 4-7b). With the Ti/Pt anode, the COD concentration was reduced by 49.6% from 2200 to 1110 mg L^{-1}. The decrease obtained with the BDD anode was 84.1%, and the COD concentration at the end of the decolorization process was only 350 mg L^{-1}. The higher removal of COD by the BDD anode could be explained by the fact that the BDD anode is inactive, whereas the Ti/Pt anode is not classed as inactive. The BDD anode has a much higher potential for oxygen evolution (2.2–2.6 V) than the Ti/Pt anode (1.7–1.9 V). Consequently, it shows higher chemical reactivity for COD oxidation (Moradi et al., 2020).

The results showed that the EO with the BDD anode did not degrade NH_4-N (Fig. 4-7a). It could be inferred that the minimal degradation of NH_4-N was mainly because of the low concentration of

hypochlorite with this anode (Chiang et al., 1995; Bagastyo et al., 2021). Ammonium is mainly degraded by oxidation with electrochemically generated hypochlorite according to reactions (4-4)–(4-10) (Chiang et al., 1995; Clifford White, 1999).

Anodic reaction: $Cl^- \rightarrow Cl_2 + 2e^-$ (4-4)

Bulk reactions: $Cl_2 + H_2O \rightarrow HOCl + H^+ + Cl^-$ (4-5)

$NH_4^+ + HOCl \rightarrow NH_2Cl + H_2O + H^+$ (4-6)

$NH_2Cl + HOCl \rightarrow NHCl_2 + H_2O$ (4-7)

$NHCl_2 + H_2O \rightarrow NOH + 2H^+ + 2Cl^-$ (4-8)

$NH_2Cl + NOH \rightarrow N_2 + HOCl + H^+ + Cl^-$ (4-9)

$2NH_4^+ + 3\mathrm{HOCl} \rightarrow N_2 + 3H_2O + 5H^+ + 3Cl^-$ (4-10)

Both the concentration of chlorine ions in the digestate and the properties of the anode affect the generation of hypochlorite in an electrochemical process. In this study, the concentration of Cl^- in SCG raw digestate was 792.5 ± 40.3 mg L^{-1} (Table 4-1). This decreased to 631.3 ± 19.6 mg L^{-1} in the liquid digestate, and then to 311. 5 ± 14.2 mg L^{-1} in the diluted digestate used for EO (two-fold dilution). Because of this low Cl^- concentration in the digestate and the fact that the BDD anode does not generate hypochlorite, degradation of ammonium ions was minimal during the EO. With the Ti/Pt anode, ammonium degradation was slightly higher than with the BDD anode because the Ti/Pt anode generated hypochlorite.

In summary, treatment of the SCG digestate by membrane filtration and EO gave a light-permeable medium with a Pt-Co value of less than 200. The resulting liquid was almost colorless and transparent (Fig. 4-8). The concentrations of NH_4-N and PO_4-P after the EO process were 520 ± 60 and 62 ± 14 mg L^{-1}, respectively. These concentrations are sufficient for microalgae cultivation (Morales-Amaral et al., 2015; Lu et al., 2022).

To evaluate the energy performance of EO of liquid digestate, the relationship (4-11) is used to calculate energy consumption (E_C) as kWh L^{-1} (Dong et al., 2021):

$$E_c = \frac{UIt}{V} \quad (4\text{-}11),$$

where U is the average voltage of the cell (V), I is the average applied current (A), t is the electrochemical reaction time (h) and V presents the volume of solution (L)

The proportion between expenses and outcome of EO should be well considered. The E_C was calculated by equation (4-11). The E_C of electrochemical decolorization of SCG liquid digestate and CM liquid digestate using the Ti/Pt anode were 278.44 kWh L^{-1} and 168.0 kWh L^{-1}, respectively. The EC of electrochemical decolorization of SCG liquid digestate using the BDD anode was 92.81 kWh L^{-1}.

In this experiment, the best performance of biogas generation from bioreactors is 4.2 L in a 28-day digestion. The methane (CH_4) content is approximately 66% determined by a gas chromatograph (GC-2014, Shimadzu, Japan), hence the capacity of CH_4 in biogas is 2.77 L. Pure methane has an energy value of 9.81 kWh L^{-1} (Eriksson, 2010). The energy content of biogas from the bioreactor is approximately 27.17 kWh.

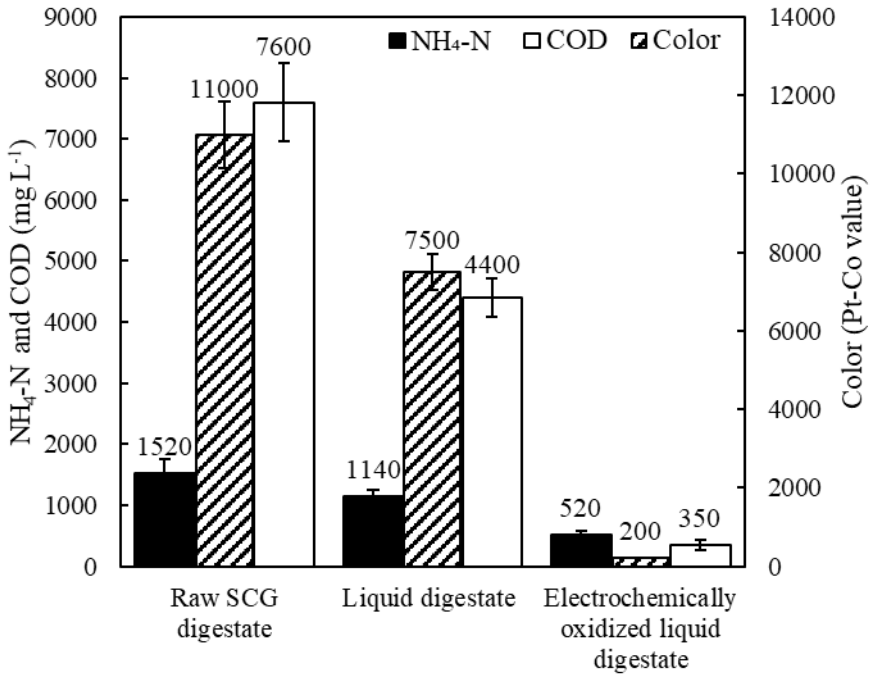

Fig. 4-6 Changes in the color (Pt-Co value), NH_4-N concentration and chemical COD in SCG, liquid digestate and electrochemically oxidized liquid digestate (two-fold dilution, n=3, Error bar: standard deviation)

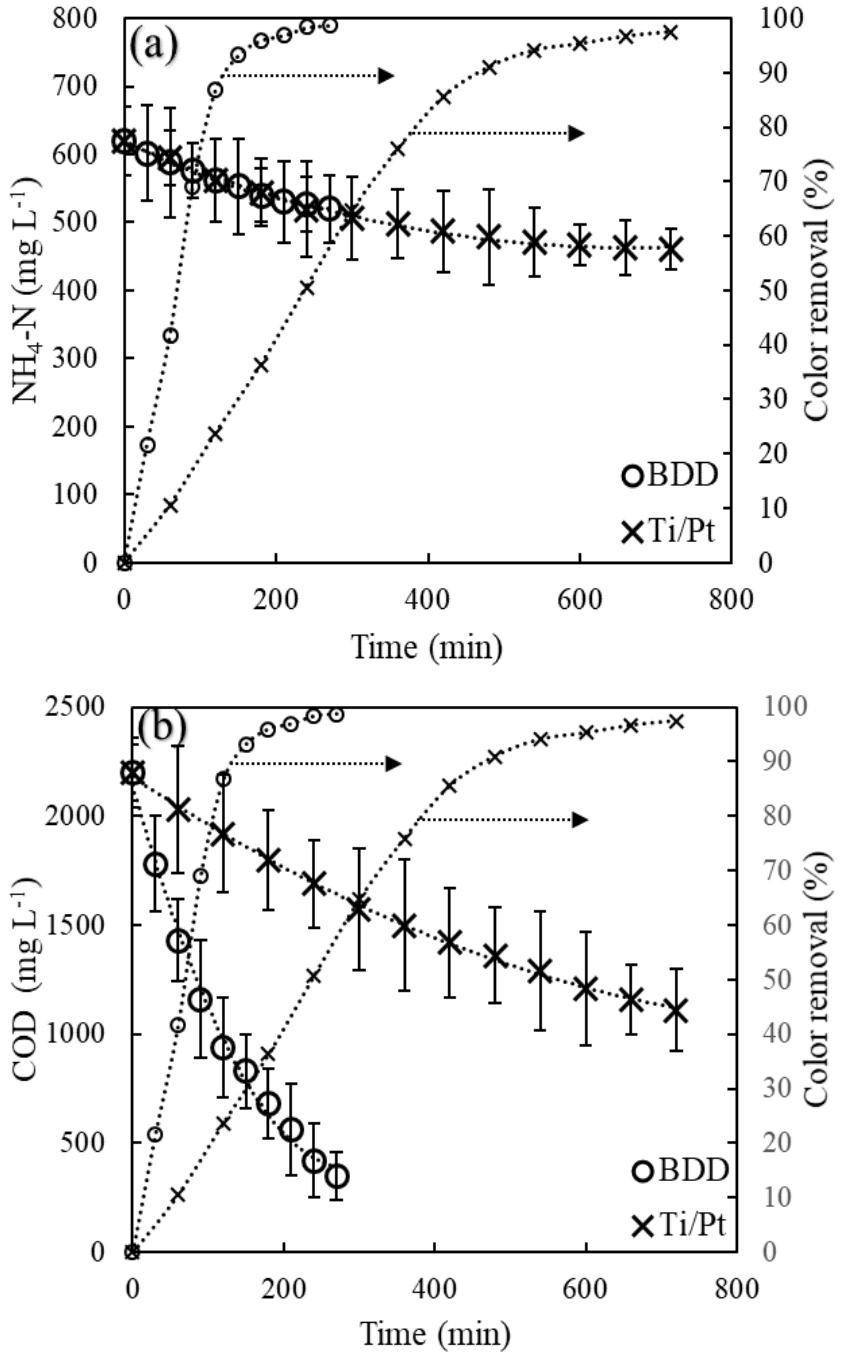

Fig. 4-7 (a) NH_4-N concentration and (b) COD removal during electrochemical decolorization (Pt-Co value of 200 at 475 nm) of SCG digestate (BDD or Ti/Pt anode, BDD cathode, current intensity 1.5 A, no addition of Fe^{2+} content, Broken line: COD and NH_4-N, Line: color removal, n=3, Error bar: standard deviation)

Fig. 4-8 Electrochemically oxidized liquid digestate with a Pt-Co value of 200

4.4 Conclusion

The EO process using a BDD anode promoted decolorization of liquid digestate from SCG and retained nutrients, especially NH_4-N. The electrochemically oxidized liquid digestate had a Pt-Co value of less than 200 and adequate NH_4-N and PO_4-P concentrations for use as a medium for cultivation of algae. The anode material affected the electrochemical decolorization of liquid digestate and the decolorization performance was in the order of Ti/IrO_2 < Ti/Pt < BDD. Increasing the initial Fe^{2+} concentration enhanced the Fenton reaction and COD removal. A higher current enhanced the electrochemical decolorization process and side reactions. The EO process removed 84.1% of the COD and retained most of the NH_4-N.

Chapter Five

Microalgae cultivation in a medium of electrochemically oxidized liquid digestate from anaerobic digestion of coffee waste biomass

This paper was published in the Journal of the Japan Institute of Energy (Chen et al., 2023)

5.1 Introduction

Biomass from microalgae has been recognized as a valuable product for biofuels (Raheem et al., 2018), feed (Spolaore et al., 2006), nutrition, and cosmetic products. Microalgae are easy to produce, with a short life cycle, high photosynthetic efficiency and a rapid growth rate. Moreover, it could use the nitrogen and phosphorus available in digestate (Morales-Amaral et al., 2015). The respective concentration of available nutrients in digestate for microalgae growth was different (ammonium 20~300 mg L^{-1}, phosphorus 5~150 mg L^{-1}) (Sayedin et al., 2020; Rajagopal et al., 2021; Kisielewska et al., 2022), but kinds of digestate have worked in microalgae cultivation. However, the high turbidity of digestate is still a major drawback of its utilization in microalgae cultivation (Monlau et al., 2015).

Anaerobic digestate contains rich nutrients, such as nitrogen and phosphorus, which could be reused in microalgae cultivation. However, a clear growth medium is required for the cultivation to facilitate light-permeable conditions. The aim of this work was to investigate microalgae cultivation in electrochemically oxidized liquid digestate from coffee waste biomass. After removing the solid fraction of the digestate through microfiltration, the liquid digestate was treated by EO using a BDD anode. The liquid digestate (LD) and electrochemically oxidized LD (ELD) were used as media for microalgae cultivation. The effects of dilution from 0 to 20 times of the LD and reaction time from 0 to 5 h of the ELD on microalgae growth were also investigated.

5.2 Materials and methods

5.2.1 Microalgae strains and pre-cultivation

The green algae *Chlorella sorokiniana* NIES-2173 was obtained from the National Institute for Environment Studies, Japan, and pre-cultivated in C-medium under continuous light illumination of 150 μmol photons m^{-2} s^{-1}. The composition of C-medium (per 100 mL) was as follows (Ichimura, 1971): 50-mg Tris(hydroxymethyl)aminomethane, 15-mg $Ca(NO_3)_2 \cdot 4H_2O$, 10-mg KNO_3, 5-mg β-Na_2glycerophosphate$\cdot 5H_2O$, 4-mg $MgSO_4 \cdot 7H_2O$, 0.01-μg Vitamin B_{12}, 0.01-μg Biotin, 1-μg thiamine HCl, and 0.3-mL PIV trace metals solution (Provasoli & Pintner, 1959): 100-mg $Na_2EDTA \cdot 2H_2O$, 19.6-mg $FeCl_3 \cdot 6H_2O$, 3.6-mg $MnCl_2 \cdot 4H_2O$, 1.04-mg $ZnCl_2$, 0.4-mg $CoCl_2 \cdot 6H_2O$, 0.25-mg $Na_2MoO_4 \cdot 2H_2O$.

5.2.2 Preparation of anaerobic digestate

The inoculum was obtained from a local wastewater treatment facility. Coffee waste was used as substrate. The reactors for digestion had a working volume of 700 mL and a total volume of 1000 mL. After the inoculum was added to the reactors, they were placed in an incubator at 37 °C for 48 h prior to the addition of substrate. The inoculum and substrate were mixed in the bottle reactor with manual shaking. The anaerobic digestion was performed with 30% headspace under a N_2 atmosphere, and the vials were closed with a butyl cap and plastic thread. The biogas is collected in a composite aluminum bag through the whole anaerobic digestion process. The anaerobic digestion experiment was carried out for 3 weeks at 37 °C. The characteristics of the anaerobic digestate from coffee waste

are shown in Table 5-1.

Table 5-1 Characteristics of the anaerobic digestate from coffee waste

Parameters	Concentrations and values
COD (mg L^{-1})	7200 ± 440
NH_4-N (mg L^{-1})	1260 ± 230
NO_2-N (mg L^{-1})	42 ± 11
TN (mg L^{-1})	1555 ± 85
TOC (mg L^{-1})	1205 ± 245
TSS (mg L^{-1})	350 ± 75
PO_4-P (mg L^{-1})	205 ± 45
Cl^- (mg L^{-1})	746 ± 50
Na^+ (mg L^{-1})	192 ± 40
K^+ (mg L^{-1})	435 ± 55
Color (Pt-Co unit)	9500 ± 750
pH	6.7 ± 0.7

5.2.3 Procedure for the pre-treatment and electrochemical oxidation treatment of digestate

A mesh filter was used to collect the liquid digestate from the anaerobic digester. Thereafter, the liquid digestate was further purified by centrifugation (4347 ×*g*, 15 min, twice) to separate suspended solids from the liquid fraction. The liquid fraction was then filtrated by a microfiltration membrane (0.2 μm), and the LD was obtained. The applied filtration unit was Vivaflow200 (Sartorius, Garman).

The filtrated digestate was treated by an EO process with BDD anode and BDD cathode. Overall electrochemical experiments were conducted in a 500 mL cylindrical reactor containing 200 mL of solution equipped with a three-piece undivided cell and a water bath to keep the solution temperature at 35 °C. It was stirred with a magnetic stirrer at 800 rpm and under a constant current condition of 1.5 A which was provided by a DC power supply (KX-100L, Takasago Electric, Inc.). The BDD plates (50 cm^2), from Sumitomo Electric Industries, were selected as the anode and cathode. The inter-electrode gap was 0.5 cm. The immersed area (35 cm^2) of each electrode was confirmed. Experimental apparatus were illustrated in Fig. 5-1.

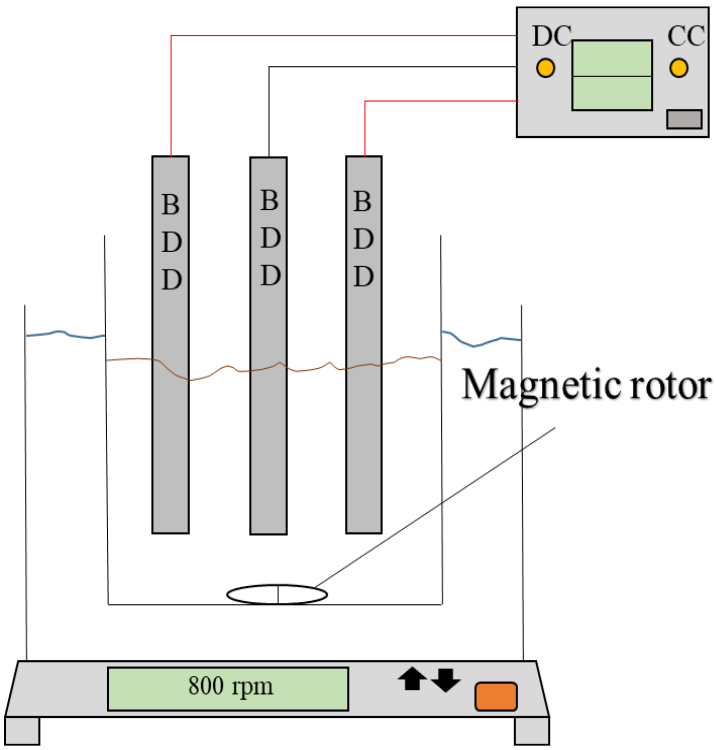

Fig. 5-1 Skeleton of experimental devices

5.2.4 Microalgae cultivation using liquid digestate and electrochemically liquid digestate

C. sorokiniana was cultivated using different media: C-medium, LD, and ELD. Cells in the exponential growth stage were used as inoculum. For microalgae cultivation, 100 mL bioreactors were used with a 20 mL medium. For the small volume cultures in this case, aeration is not necessary, because the applied bioreactors were with air permeable caps. Temperature and light intensity were maintained at 25 ± 1 °C and 150 μmol photons m^{-2} s^{-1} (10/14 Light/Dark, cycle: 24 h), respectively. The cultures were mixed thoroughly by shaking every 3 or 4 d, and optical density (OD) at a wavelength of 680 nm which is the absorbance at 680 nm and cell density were measured each time. The nutrient concentrations were determined before and after cultivation. Dilution of digestate was required for microalgae cultivation, primarily, to increase light permeability. The microalgae cultivation was carried out in 0 to 20 times dilution media. The reaction time of EO is an important parameter for improving the light permeability into digestate media (Gonçalves et al., 2012). Batch cultivation of *C. sorokiniana* NIES-2173 was conducted using 0 (LD), 1, 2, 3, 4 and 5 h ELD.

5.2.5 Analytic methods

Color density at a wavelength of 475 nm, which is the absorbance at 475 nm, of solutions was determined with a UV-vis spectrophotometer (U-5100, HITACHI, Japan). The color removal was calculated by Eq. (5-1), based on the determined absorbance at a certain wavelength (475 nm):

$$\%\text{Color removal} = \frac{A_0 - A}{A_0} * 100 \qquad (5\text{-}1),$$

where A_0 and A refer to the simple absorbance at the initial time and at a given time during the electrochemical process, respectively. The OD of the microalgae culture was calculated by subtracting

the OD of a control medium (medium with no microalgae) from the OD of the microalgae culture in the medium to account for the color of the medium and the presence of bacteria. Microalgae cell density (cell number) was also determined by a light microscope. The calibration curve of Pt-Co unit and absorbance of solutions (color density) was calibrated with 100 and 1000 Pt-Co unit color standard solutions (Cardoso et al. 2016; Sathishkumar et al. 2017). Color density was analyzed according to the American Dye Manufactures' Institute (ADMI) method (APHA Method 2120 F, 2017).

The specific growth rate of *Chlorella sorokiniana* was calculated using Equation (5-2):

$$\mu = \frac{\ln(\frac{x_2}{x_1})}{t_2 - t_1} \qquad (5\text{-}2),$$

where μ is specific growth rate (d^{-1}), x_1 and x_2 are the OD at 680 nm (-) at time t_1 and t_2 (d), respectively.

The analyses of all parameters were conducted according to the Standard Method for Examination of Water and Wastewater (APHA, 2017). The COD and PO_4^{3-} concentrations were measured using a spectrometer (DR3900, HACH, USA) and their respective methods. Cations (NH_4^+, Na^+, K^+, Ca^{2+} and Mg^{2+}) and anions (Cl^-, NO_2^-, NO_3^- and PO_4^{3-}), were determined using an ion-chromatography system (IC-8100, TOSOH, Japan). The TN and TOC were measured by a TN and TOC analyzer (TNM-L, TOC-L, SHIMADZU, Japan).

5.3 Results and Discussion

5.3.1 Electrochemical oxidation of liquid digestate

Fig. 5-2 illustrates the variation of color density (absorbance) at 475 nm and ammonium concentration with reaction time during EO of LD using BDD anode and cathode under 1.5 A of current intensity. The LD solution quickly lost its color and became colorless, with an approximate clear state after 180 min, achieving about 85% color decay (Fig. 5-2). The nature of the non-active anode BDD which has higher electrocatalytic activity to generate reactive oxidizing species, such as ·OH, on its surface (Panizza & Cerisola, 2005), may explain the above results. This could be accounted for by the wide electrochemical window of the BDD anode, which may cause the anode to produce large quantities of ·OH radicals and other active species (Fernandes et al., 2015). The COD concentration was also reduced by the intensive oxidation and the COD removal rate was as high as 82% (5470 ± 450 to 980 ± 75 mg L^{-1}).

The concentration of ammonium ions only declined by 19% after 3 h EO with the BDD anode. It is clear from Fig. 5-2 that the EO process did not effectively degrade NH_4-N. This limited removal of ammonium was mainly due to the small amount of hypochlorite. It is well known that most ammonium degradation is mainly due to the oxidation effect of hypochlorite (Bagastyo et al., 2021). The concentration of chlorine ions and the anodic property of chlorine evolution have an effect on the production of hypochlorite by an electrochemical process (Ihara et al., 2006). It indicated that the low Cl^- concentration in ELD (328.7 ± 17.4 mg L^{-1}) may cause little hypochlorite to be electrochemically generated, and consequently, a smaller reduction of ammonium ions during the electrochemical process (Chiang et al., 1995). The concentration of PO_4-P did not change significantly, 74 ± 8 mg L^{-1} was kept during EO. It might be attributed to the fact that PO_4-P could not be

electrochemically oxidized, but could be removed by physical methods like precipitation, filtration, and adsorption (Bunce et al., 2018). Moreover, the biological method including microalgae cultivation could recover PO_4-P.

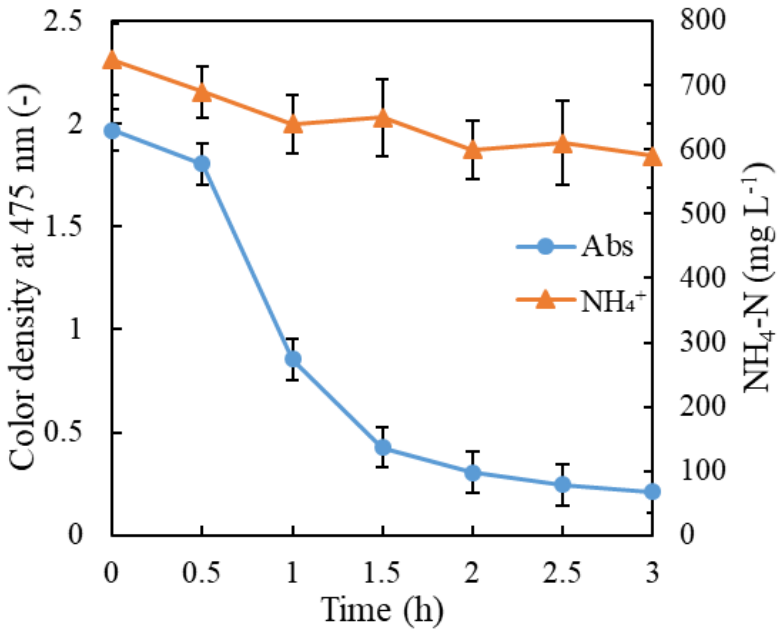

Fig. 5-2 Color density (absorbance) and change in ammonium concentration *versus* reaction time for EO of LD with BDD anode and BDD cathode (current intensity 1.5 A, no addition of Fe^{2+}, n=3, Error bar: standard deviation)

5.3.2 Effect of dilution of liquid digestate on microalgae cultivation

Fig. 5-3 shows the effect of the dilution ratio of LD on microalgae cultivation. After 21 d cultivation, algae in 10 times diluted LD grew by the largest additional OD of 0.976 (-) (specific growth rate of 0.53 ± 0.07 d^{-1}) and had the highest cell density of 8.4×10^6 cells ml^{-1}. Although there was a lag in the condition of 5 times dilution, it could still be concluded that this strain of microalgae could acclimate itself to the medium and grow well under moderate conditions.

Fig. 5-3(a) and (b) showed a similar trend, there was no significant increase in OD at 680 nm and cell density in the LD without dilution. It might be accounted for the fact that the medium was not light permeable with a high color density at 475nm (more than 2.20(-)), and thus restrained microalgal growth (Cheunbarn & Peerapornpisal, 2010). The condition of 20 times dilution obtained a fast increase in the first 3 d cultivation. However, it decreased quickly and reached a final cell density of 8.0×10^6 cells ml^{-1} which was lower than the condition of 10 times dilution. The 20 times diluted LD had the lowest initial color density at 475 nm and the lowest initial COD concentration in all conditions. The removal rate of COD during cultivation was more than 97% (from 273 ± 22 to 267 ± 13 mg L^{-1}). Carbon is an essential source of microalgal growth (Ma et al., 2022). It indicated that the organic carbon source in 20 times diluted LD might be not sufficient for the 21 d cultivation.

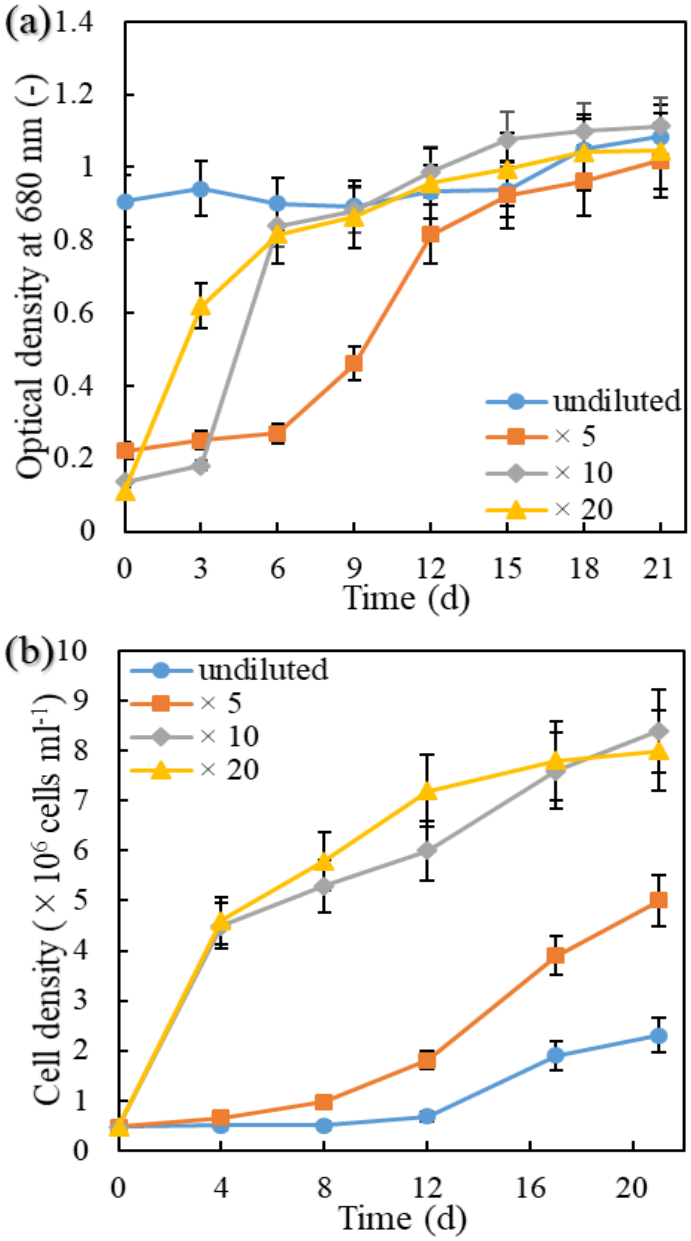

Fig. 5-3 Effect of dilution ratio (× times) of LD on microalgae cultivation reflected by the OD at 680 nm (a) and cell density (b) (n=3, Error bar: standard deviation)

5.3.3 Effect of reaction time of electrochemical oxidation of liquid digestate on microalgae cultivation

Fig. 5-4 shows the effect of reaction time on EO of LD on microalgae cultivation. The growth rates within the first 3 d were similar from 2 to 5 h conditions and 0 to 1 h conditions had the same growth rates. They declined gradually throughout the cultivation period, with a final OD at 680 nm that was 0.712 to 1.27 (-). By the initial color density at 475 nm, the LD with the highest initial color density at 475 nm (1.97 (-)) decreased the growth rate by 50% compared with the 2 h ELD, while the 2 h and 3 h ELD with lower initial color densities (0.305, 0.211 (-)) achieved the highest specific growth rates of 0.79 ± 0.11 and 0.78 ± 0.13 d^{-1}, respectively. The 21 d cultivation in 2 h ELD obtained the largest cell density of 1.28×10^7 cells ml^{-1} (Fig. 5-4b). It indicated that the 2 h ELD was effective for use as a medium in microalgae cultivation, which might be attributed to the higher light permeability for photosynthesis (Wang et al., 2014).

The 4 h and 5 h conditions had a lower initial color density at 475 nm, and the specific growth rate and final cell density were lower than in the 2 h conditions. As the EO reaction time increased, the pH increased from 7.6 ± 0.2 to 8.7 ± 0.3, meanwhile, the concentration of NH_4-N decreased from 740 mg L^{-1} to 530 mg L^{-1}. The optimum pH for growth of *C. sorokiniana* was around 7.0 (Zheng et al., 2013), and the higher initial pH was obtained by conditions of 4 h and 5 h. Their specific growth rates (0.71 ± 0.09 and 0.73 ± 0.11 d^{-1} for 4 h and 5 h, respectively) and final cell densities were lower than those of the 2 h condition. It is worth mentioning that the concentrations of PO_4-P slightly decreased after 3 h EO, which may be caused by precipitation owing to the higher pH (which exceeded 8.0) (McGriff & McKinney 1972; Song et al., 2002).

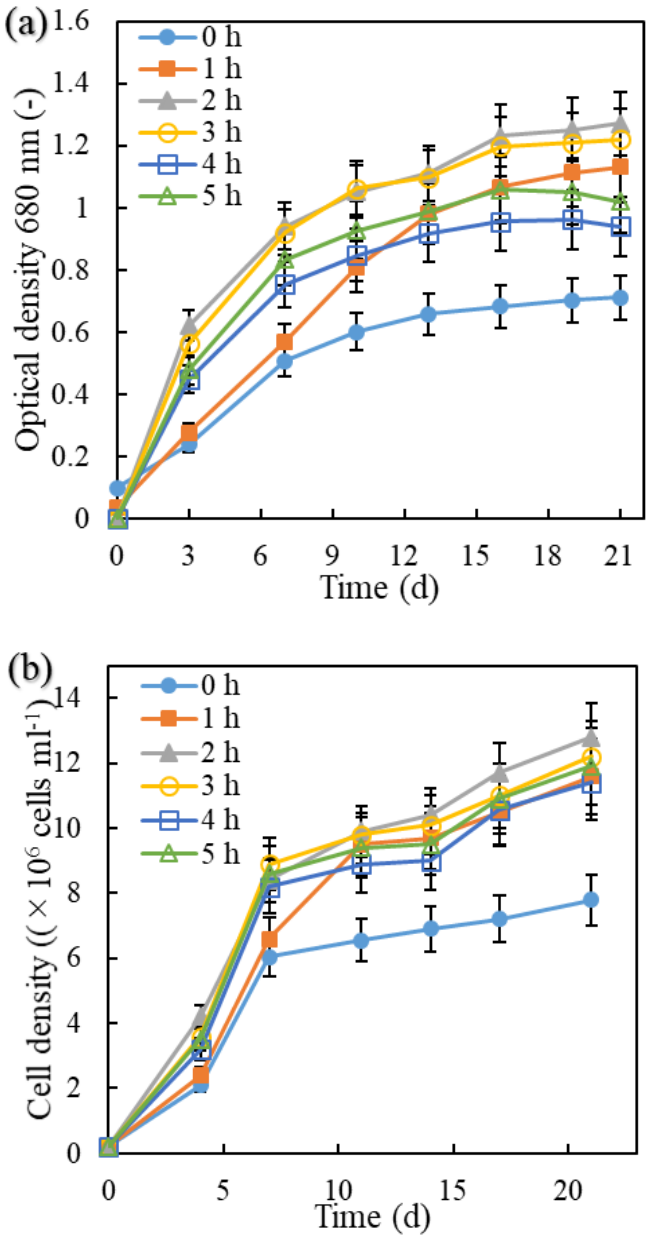

Fig. 5-4 Effect of reaction time of EO of LD on microalgae cultivation reflected by the OD at 680 nm (a) and cell density (b) (BDD anode, current intensity 1.5 A, n=3, Error bar: standard deviation)

5.3.4 Microalgae cultivation in the media of liquid digestate and electrochemically oxidized liquid digestate

Fig. 5-5 depicts the performance of batch cultivation of *C. sorokiniana* NIES-2173 using LD and 2 h ELD with 0, 5 and 10 times dilution. After 28 d cultivation, the growth of microalgae was all positive using six media. The 10 times diluted ELD showed the best performance among the six media, and it only lowered the specific growth rate by 10% compared with the C-medium. Owing to the lower color density (Monlau et al., 2015) at 475 nm after dilution, it achieved a higher specific growth rate and final cell density than in the condition of ELD without dilution. This could also explain the results of a series of LDs.

The growth rate of 10 times diluted LD was faster than that of 10 times diluted ELD in the first 7 d cultivation, whereas the contrary result was obtained from the 7th day to the end of cultivation. The ELD without dilution achieved a higher specific growth rate and final cell density than the same condition of LD without dilution, and even higher than 10 times diluted LD. According to the findings in Fig. 5-5, ELD as a light permeable medium is more likely to contribute to microalgae cultivation than LD medium, and the removal rates of NH_4-N, PO_4-P and COD in Table 5-2 demonstrated the results. This is mainly due to the higher light permeability of ELD (Table 5-2).

After 21 d cultivation, a part of NH_4-N and PO_4-P remained in all conditions (Fig. 5-6). The growth of *C. sorokiniana* in conditions using LD and ELD media may be restrained by light control, pH changes, and/or a deficiency of dissolved inorganic carbon, trace metals, and other micronutrients (Sekine et al., 2020), instead of NH_4-N and PO_4-P limitation. The data in Table 5-2 and Fig. 5-6 also indicated that the specific growth rate and final cell density might be not significantly affected by differences in nutrient concentration while being mainly affected by initial color density at 475 nm in this batch of cultivation. From Table 5-2, the data on nutrients and COD removal rates were comparable to, if not better than, those of other researches (Sekine et al. 2020; Gupta et al. 2016;

Kobayashi et al. 2013; Ramsundar et al. 2017).

The proportion between expenses and outcome of EO should be well considered. The E_C was calculated by equation (4-11). The E_C of electrochemical decolorization of LD using the BDD anode and BDD cathode was 165.0 kWh L^{-1}.

The best performance of biogas generation from bioreactors is 3.8 L in a 21-day digestion. The methane (CH_4) content is approximately 64% measured by a gas chromatograph (GC-2014, Shimadzu, Japan), hence the capacity of CH_4 in biogas is 2.43 L. Pure methane has an energy value of 9.81 kWh L^{-1} (Eriksson, 2010). The energy content of biogas from the bioreactor is approximately 23.84 kWh.

Table 5-2 Initial color density at 475 nm and nutrient removal in LD and ELD media with conditions

	Color density at 475 nm	Removal rate of NH_4-N	Removal rate of PO_4-P	The removal rate of COD
undiluted ELD	0.305	0.52	0.86	0.83
× 5 ELD	0.090	0.58	0.79	0.87
× 10 ELD	0.034	0.49	0.89	0.92
undiluted LD	1.970	0.08	0.20	0.29
× 5 LD	0.745	0.51	0.67	0.56
× 10 LD	0.300	0.53	0.73	0.86

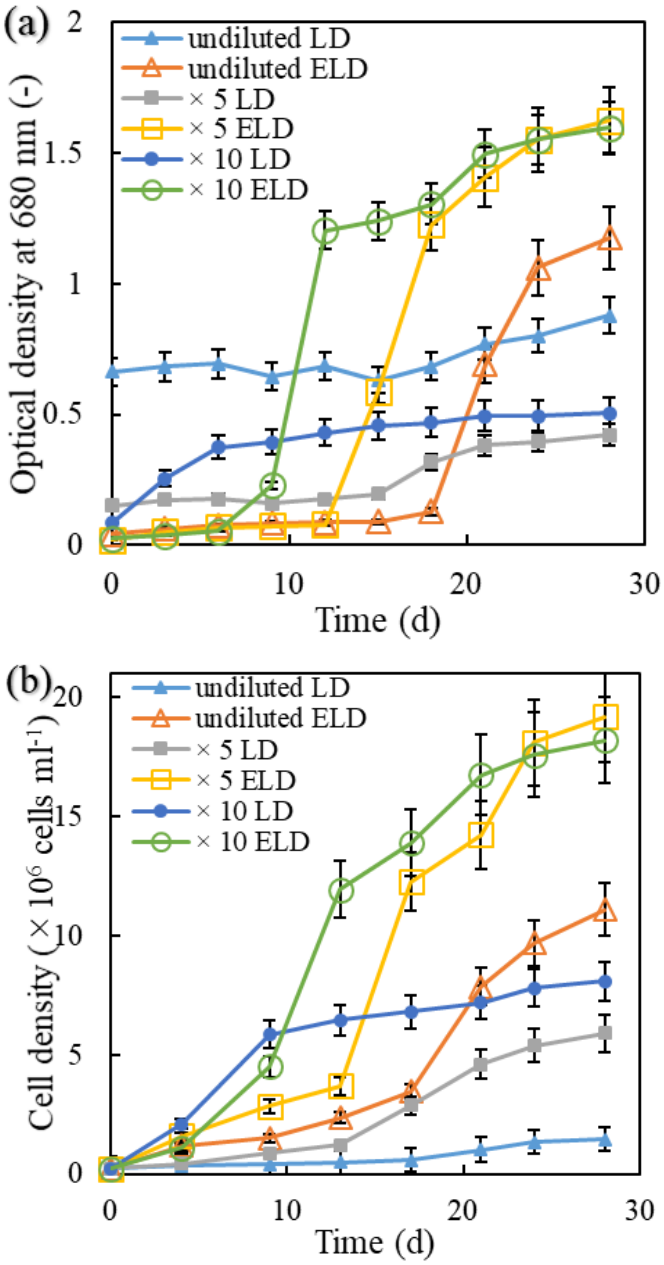

Fig. 5-5 The growth of *Chlorella sorokiniana* (OD at 680 nm (a) and cell density (b) *versus* cultivation time) in the media of LD and ELD with different dilution (× times) and reaction time correspondingly (BDD anode, current intensity 1.5 A, n=3, Error bar: standard deviation)

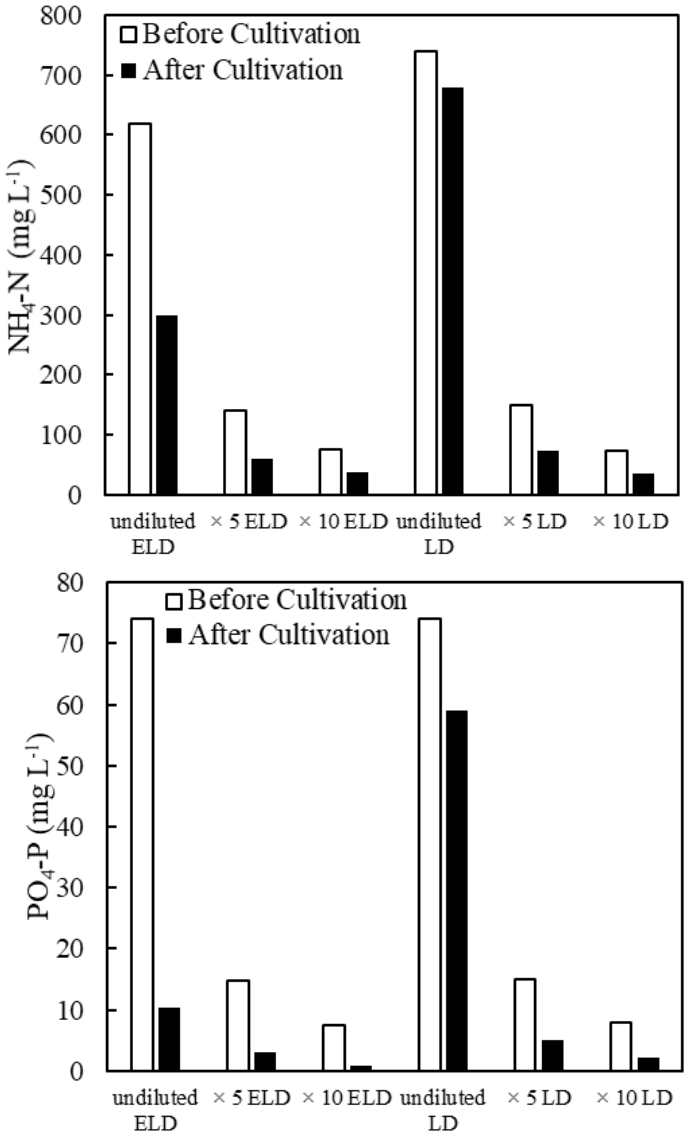

Fig. 5-6 NH_4-N and PO_4-P concentrations of LD and ELD media with conditions before (hollow bar) and after (filled bar) *C. sorokiniana* NIES-2173 cultivation

5.4 Conclusion

Using BDD anode, EO effectively decolorized LD (highest 85% color removal with a color density of 0.3 (-) at 475 nm) while retaining the majority of NH_4-N (80%) and PO_4-P (99%) content. For the cultivation, 10 times diluted LD achieved the highest specific growth rate and final cell density among 0 to 20 times dilutions, which may account for the higher light permeability and sufficient organic carbon source. The reaction time of EO had a significant effect on microalgae cultivation. In 0 to 5 h EO treatment, 2 h ELD obtained the best results in terms of microalgal growth. It indicated that except for the necessary light permeable condition, other conditions like pH and variation in nutrients also had an effect on the cultivation.

Attributed to the higher light permeability and more adequate configuration of nutrients, the 10 times diluted, 2 h ELD achieved the best cultivation performance in all conditions. As a result of cultivating *C. sorokiniana* NIES-2173 using different growth media, the final biomass concentration (OD at 680 nm) and cell density were lower using LD compared with ELD. In contrast, better growth of *C. sorokiniana* was obtained using ELD even without dilution, indicating that ELD as a highly light-permeable medium was more effective for microalgae cultivation.

Chapter Six
Conclusion

To construct an upcycling of food waste, a liquid digestate with excellent light permeability was prepared by combining anaerobic digestion and electrochemical oxidation, and its potential as a microalgae culture medium was evaluated.

1) Food colorants always remain in food waste. Aqueous solutions containing Caramel Class IV, Caramel Class III, and AO7 were decolorized almost completely by EAOPs, including EO, EF, and EO+EF using BDD and Ti/Pt electrodes under an experimental optimized condition. It indicated that electrochemical oxidation is effective in the decolorization of different food colorants.
2) The food waste such as coffee waste is practicable for anaerobic digestion. The EO process using BDD anodes promoted the decolorization of liquid digestate from coffee waste biomass and retained nutrients, especially NH_4-N. The electrochemically oxidized liquid digestate had a significantly low Pt-Co value and adequate NH_4-N and PO_4-P concentrations. It indicated that this light-permeable liquid digestate is feasible to be used as a medium for the cultivation of algae.
3) As a result of cultivating *Chlorella* sorokiniana NIES-2173 using different growth media, the LD had a fairly lower final biomass concentration and cell density than the ELD. Although the initial color density was almost the same, the undiluted ELD still achieved a higher final productivity of the microalgae than that of the diluted LD. This indicated that the ELD as a highly light-permeable medium is more effective for microalgae cultivation.
4) The data of changes in the nutrients during cultivation and biomass production from the use of the ELD medium achieved the comparable to, if not better than, those of other researches. It can be attributed to the higher light permeability and more appropriate configuration of

nutrients.

These findings show that the EO process is practicable to decolorize the colorants and liquid digestate with high turbidity, which is available to produce highly light-permeable media with adequate nutrients for microalgae cultivation. The establishment of a combining process will contribute to the prevention of environmental pollution and upcycling of food waste.

References

Ahmad, T., Ahmad, K., & Alam, M. (2017). Sludge quantification at water treatment plant and its management scenario. *Environmental Monitoring and Assessment*, *189*(9). https://doi.org/10.1007/s10661-017-6166-1

Akhiar, A., Battimelli, A., Torrijos, M., & Carrere, H. (2017). Comprehensive characterization of the liquid fraction of digestates from full-scale anaerobic co-digestion. *Waste Management*, *59*, 118–128. https://doi.org/10.1016/j.wasman.2016.11.005

Aksu, Z. (2001). Equilibrium and kinetic modelling of iron adsorption by eggshells in a batch system: effect of temperature. *Separation and Purification Technology*, *21*, 285–294. https://doi.org/https://doi.org/10.1016/S1383-5866(00)00212-4

Albiach, R., Canet, R., Pomares, F., & Ingelmo, F. (2000). Microbial biomass content and enzymatic activities after the application of organic amendments to a horticultural soil. *Bioresource Technology*, *75*(1), 43–48. https://doi.org/10.1016/S0960-8524(00)00030-4

APHA (2017). Standard methods for the examination of water and wastewater, 23rd edn. Washington DC.

APHA Method 2120 F (2017). ADMI Weighted-Ordinate Spectrophotometric Method. In *Standard methods for the examination of water and wastewater, 21th edn* (pp. 234). APHA. Washington DC.

Bagastyo, A. Y., Hidayati, A. S., Herumurti, W., & Nurhayati, E. (2021). Application of boron-doped diamond, Ti/IrO_2, and Ti/Pt anodes for the electrochemical oxidation of landfill leachate biologically pretreated by moving bed biofilm reactor. *Water Science and Technology*, *83*(6), 1357–1368. https://doi.org/10.2166/wst.2021.060

Bchir, F. S., Gannoun, H., Herry, S. El, & Hamdi, M. (2011). Optimization of Spongiochloris sp. biomass production in the abattoir digestate. *Bioresource Technology*, *102*(4), 3869–3876. https://doi.org/10.1016/j.biortech.2010.11.036

Bedolla-Guzman, A., Sirés, I., Thiam, A., Peralta-Hernández, J. M., Gutiérrez-Granados, S., & Brillas, E. (2016). Application of anodic oxidation, electro-Fenton and UVA photoelectro-Fenton to decolorize and mineralize acidic solutions of Reactive Yellow 160 azo dye. *Electrochimica Acta*, *206*, 307–316. https://doi.org/10.1016/j.electacta.2016.04.166

Beuckels, A., Smolders, E., & Muylaert, K. (2015). Nitrogen availability influences phosphorus removal in microalgae-based wastewater treatment. *Water Research*, *77*, 98–106. https://doi.org/10.1016/j.watres.2015.03.018

Bich, N. N., Yaziz, M. I., & Bakti, N. A. K. (1999). Combination of Chlorella vulgaris and

Eichhornia crassipes for wastewater nitrogen removal. *Water Research*, *33*(10), 2357–2362. https://doi.org/10.1016/S0043-1354(98)00439-4

Brillas, E., Sirés, I., & Oturan, M. A. (2009). Electro-fenton process and related electrochemical technologies based on fenton's reaction chemistry. *Chemical Reviews*, *109*(12), 6570–6631. https://doi.org/10.1021/cr900136g

Bunce, J. T., Ndam, E., Ofiteru, I. D., Moore, A., & Graham, D. W. (2018). A review of phosphorus removal technologies and their applicability to small-scale domestic wastewater treatment systems. *Frontiers in Environmental Science*, *6*(FEB), 1–15. https://doi.org/10.3389/fenvs.2018.00008

Caetano, N. S., Silva, V. F. M., Melo, A. C., Martins, A. A., & Mata, T. M. (2014). Spent coffee grounds for biodiesel production and other applications. *Clean Technologies and Environmental Policy*, *16*(7), 1423–1430. https://doi.org/10.1007/s10098-014-0773-0

Cardoso, J. C., Bessegato, G. G., & Boldrin Zanoni, M. V. (2016). Efficiency comparison of ozonation, photolysis, photocatalysis and photoelectrocatalysis methods in real textile wastewater decolorization. *Water Research*, *98*, 39–46. https://doi.org/10.1016/j.watres.2016.04.004

Chen, H.B., Yoshida, G., Fetra, J. A., Ihara, I. (2022). Electro-oxidation combined with electro-Fenton for decolorization of caramel colorant aqueous solution using BDD electrodes. *Journal of Water Process Engineering*, *47*, 102672. https://doi.org/10.1016/j.jwpe.2022.102672

Chen, H.B., Yoshida, G., Fetra, J. A., Ihara, I. (2023): Microalgae Cultivation in Electrochemically Oxidized Anaerobic Digestate from Coffee Waste Biomass. *Journal of the Japan Institute of Energy*, *102*, 96-103. https://doi.org/10.3775/jie.102.96

Chen, R., Li, R., Deitz, L., Liu, Y., Stevenson, R. J., & Liao, W. (2012). Freshwater algal cultivation with animal waste for nutrient removal and biomass production. *Biomass and Bioenergy*, *39*, 128–138. https://doi.org/10.1016/j.biombioe.2011.12.045

Cheunbarn, S., & Peerapornpisal, Y. (2010). Cultivation of Spirulina platensis using anaerobically swine wastewater treatment effluent. *International Journal of Agriculture and Biology*, *12*(4), 586–590. https://doi.org/10–144/AWB/2010/12–4–586–590

Chiang, L. C., Chang, J. E., & Wen, T. C. (1995). Indirect oxidation effect in electrochemical oxidation treatment of landfill leachate. *Water Research*, *29*(2), 671–678. https://doi.org/10.1016/0043-1354(94)00146-X

Clifford White, G. (1999) Chemistry of chlorination. In Clifford White G (Ed.), *Handbook of chlorination and alternative disinfectants, 4th edn* (pp. 231-247).Wiley. New York.

Cruz-González, K., Torres-Lopez, O., García-León, A. M., Brillas, E., Hernández-Ramírez, A., & Peralta-Hernández, J. M. (2012). Optimization of electro-Fenton/BDD process for

decolorization of a model azo dye wastewater by means of response surface methodology. *Desalination*, *286*, 63–68. https://doi.org/10.1016/j.desal.2011.11.005

Dang, N. M., & Lee, K. (2018). Decolorization of organic fertilizer using advanced oxidation process and its application for microalgae cultivation. *Journal of Industrial and Engineering Chemistry*, *59*, 297–303. https://doi.org/10.1016/j.jiec.2017.10.035

Dong, P., Wang, H., Liu, W., Wang, S., Wang, Y., Zhang, J., Lin, F., Wang, Y., Zhao, C., Duan, X., Wang, S., & Sun, H. (2021). Quasi-MOF derivative-based electrode for efficient electro-Fenton oxidation. *Journal of Hazardous Materials*, *401*(April 2020), 123423. https://doi.org/10.1016/j.jhazmat.2020.123423

Duarte, J. L. da S., Solano, A. M. S., Arguelho, M. L. P. M., Tonholo, J., Martínez-Huitle, C. A., & Zanta, C. L. de P. e. S. (2018). Evaluation of treatment of effluents contaminated with rifampicin by Fenton, electrochemical and associated processes. *Journal of Water Process Engineering*, *22*(March), 250–257. https://doi.org/10.1016/j.jwpe.2018.02.012

El-Ghenymy, A., Centellas, F., Rodríguez, R. M., Cabot, P. L., Garrido, J. A., Sirés, I., & Brillas, E. (2015). Comparative use of anodic oxidation, electro-Fenton and photoelectro-Fenton with Pt or boron-doped diamond anode to decolorize and mineralize Malachite Green oxalate dye. *Electrochimica Acta*, *182*, 247–256. https://doi.org/10.1016/j.electacta.2015.09.078

Eriksson, O. (2010). Environmental Technology Assessment of Natural Gas Compared to Biogas. In P. Potocnik (Ed.), *Natural Gas* (pp. 128–146). InTech. https://doi.org/10.5772/9837

Ertugay, N., & Acar, F. N. (2017). Removal of COD and color from Direct Blue 71 azo dye wastewater by Fenton's oxidation: Kinetic study. *Arabian Journal of Chemistry*, *10*(February), S1158–S1163. https://doi.org/10.1016/j.arabjc.2013.02.009

FAO (2011). Caramel Colours. *Food and Agriculture Orgnazation*. https://www.fao.org/fileadmin/user_upload/jecfa_additives/docs/monograph11/additive-102-m11.pdf

Fernandes, A., Pacheco, M. J., Ciríaco, L., & Lopes, A. (2015). Review on the electrochemical processes for the treatment of sanitary landfill leachates: Present and future. *Applied Catalysis B: Environmental*, *176–177*, 183–200. https://doi.org/10.1016/j.apcatb.2015.03.052

Franchino, M., Comino, E., Bona, F., & Riggio, V. A. (2013). Growth of three microalgae strains and nutrient removal from an agro-zootechnical digestate. *Chemosphere*, *92*(6), 738–744. https://doi.org/10.1016/j.chemosphere.2013.04.023

Garcia-Segura, S., Centellas, F., Arias, C., Garrido, J. A., Rodríguez, R. M., Cabot, P. L., & Brillas, E. (2011). Comparative decolorization of monoazo, diazo and triazo dyes by electro-Fenton process. *Electrochimica Acta*, *58*(1), 303–311. https://doi.org/10.1016/j.electacta.2011.09.049

Girotto, F., Pivato, A., Cossu, R., Nkeng, G. E., & Lavagnolo, M. C. (2018). The broad spectrum of

possibilities for spent coffee grounds valorisation. *Journal of Material Cycles and Waste Management*, *20*(1), 695–701. https://doi.org/10.1007/s10163-017-0621-5

Gonçalves, M. R., Marques, I. P., & Correia, J. P. (2012). Electrochemical mineralization of anaerobically digested olive mill wastewater. *Water Research*, *46*(13), 4217–4225. https://doi.org/10.1016/j.watres.2012.05.019

Gupta, S. K., Ansari, F. A., Shriwastav, A., Sahoo, N. K., Rawat, I., & Bux, F. (2016). Dual role of Chlorella sorokiniana and Scenedesmus obliquus for comprehensive wastewater treatment and biomass production for bio-fuels. *Journal of Cleaner Production*, *115*, 255–264. https://doi.org/10.1016/j.jclepro.2015.12.040

Hadiyanto, H., Christwardana, M., & Soetrisnanto, D. (2013). Phytoremediations of Palm Oil Mill Effluent (POME) by using aquatic plants and microalge for biomass production. *Journal of Environmental Science and Technology*, *6*(2), 79–90. https://doi.org/10.3923/jest.2013.79.90

Huo, S., Necas, D., Zhu, F., Chen, D., An, J., Zhou, N., Liu, W., Wang, L., Cheng, Y., Liu, Y., & Ruan, R. (2021). Anaerobic digestion wastewater decolorization by H_2O_2-enhanced electro-Fenton coagulation following nutrients recovery via acid tolerant and protein-rich Chlorella production. *Chemical Engineering Journal*, *406*(September 2020), 127160. https://doi.org/10.1016/j.cej.2020.127160

Huo, S., Wang, Z., Zhu, S., Shu, Q., Zhu, L., Qin, L., Zhou, W., Feng, P., Zhu, F., Yuan, Z., & Dong, R. (2018). Biomass accumulation of Chlorella zofingiensis G1 cultures grown outdoors in photobioreactors. *Frontiers in Energy Research*, *6*(JUN), 1–8. https://doi.org/10.3389/fenrg.2018.00049

Huo, S., Zhu, F., Zou, B., Xu, L., Cui, F., & You, W. (2018). A two-stage system coupling hydrolytic acidification with algal microcosms for treatment of wastewater from the manufacture of acrylonitrile butadiene styrene (ABS) resin. *Biotechnology Letters*, *40*(4), 689–696. https://doi.org/10.1007/s10529-018-2513-8

Ichimura, T. (1971). Sexual cell division and conjugation-papilla formation in sexual reproduction of Closterium strigosum. In *Proceedings of the Seventh international Seaweed Symposium* (pp. 208–214). University of Tokyo Press. Tokyo.

Ihara, I., Umetsu, K., Kanamura, K., & Watanabe, T. (2006). Electrochemical oxidation of the effluent from anaerobic digestion of dairy manure. *Bioresource Technology*, *97*(12), 1360–1364. https://doi.org/10.1016/j.biortech.2005.07.007

Kishimoto, N., Minakata, D., & Somiya, I. (2005). Effects of hydrodynamic conditions on OH radical production at Ti/Pt anodes during electrochemical treatment. *Environmental Technology*, *26*(10), 1161–1172. https://doi.org/10.1080/09593332608618480

Kisielewska, M., Dębowski, M., Zieliński, M., Kazimierowicz, J., Quattrocelli, P., & Bordiean, A. (2022). Effects of Liquid Digestate Treatment on Sustainable Microalgae Biomass Production.

BioEnergy Research, *15*(1), 357–370. https://doi.org/10.1007/s12155-021-10251-x

Kobayashi, N., Noel, E. A., Barnes, A., Watson, A., Rosenberg, J. N., Erickson, G., & Oyler, G. A. (2013). Characterization of three Chlorella sorokiniana strains in anaerobic digested effluent from cattle manure. *Bioresource Technology*, *150*, 377–386. https://doi.org/10.1016/j.biortech.2013.10.032

Krzemińska, D., Neczaj, E., & Borowski, G. (2015). Advanced oxidation processes for food industrial wastewater decontamination. *Journal of Ecological Engineering*, *16*(2), 61–71. https://doi.org/10.12911/22998993/1858

Kulandaivelu, V., & Bhat, R. (2012). Changes in the physico-chemical and biological quality attributes of soil following amendment with untreated coffee processing wastewater. *European Journal of Soil Biology*, *50*, 39–43. https://doi.org/10.1016/j.ejsobi.2011.11.011

Lane, A. G. (1983). Anaerobic digestion of spent coffee grounds. *Biomass*, *3*(4), 247–268. https://doi.org/10.1016/0144-4565(83)90017-3

Liakos, T. I., Sotiropoulos S., Lazaridis N.K. (2017) Electrochemical and bio-electrochemical treatment of baker's yeast effluents. *Journal of Environmental Chemical Engineering* 5, 699–708. https://doi.org/https://doi.org/10.1016/j.jece.2016.12.048

Lim, S. L., Chu, W. L., & Phang, S. M. (2010). Use of Chlorella vulgaris for bioremediation of textile wastewater. *Bioresource Technology*, *101*(19), 7314–7322. https://doi.org/10.1016/j.biortech.2010.04.092

Ltaïef, A. H., Sabatino, S., Proietto, F., Ammar, S., Gadri, A., Galia, A., & Scialdone, O. (2018). Electrochemical treatment of aqueous solutions of organic pollutants by electro-Fenton with natural heterogeneous catalysts under pressure using Ti/IrO_2-Ta_2O_5 or BDD anodes. *Chemosphere*, *202*, 111–118. https://doi.org/10.1016/j.chemosphere.2018.03.061

Lu, R., Yan, H., Liu, Y., Wang, Y., Cui, X., Wu, X., Yu, Z., Ruan, R., & Zhang, Q. (2022). Enhancement of nutrients recovery and cell metabolism in piggery anaerobic digestate by the co-cultivation of indigenous microalgae and bacteria. *Journal of Cleaner Production*, *375*(April), 134193. https://doi.org/10.1016/j.jclepro.2022.134193

Luz, F. C., Cordiner, S., Manni, A., Mulone, V., & Rocco, V. (2017). Anaerobic Digestion of Liquid Fraction Coffee Grounds at Laboratory Scale: Evaluation of the Biogas Yield. *Energy Procedia*, *105*, 1096–1101. https://doi.org/10.1016/j.egypro.2017.03.470

Ma, X., Mi, Y., Zhao, C., & Wei, Q. (2022). A comprehensive review on carbon source effect of microalgae lipid accumulation for biofuel production. *Science of the Total Environment*, *806*, 151387. https://doi.org/10.1016/j.scitotenv.2021.151387

Mandal, P., Dubey, B. K., & Gupta, A. K. (2017). Review on landfill leachate treatment by electrochemical oxidation: Drawbacks, challenges and future scope. *Waste Management*, *69*,

250–273. https://doi.org/10.1016/j.wasman.2017.08.034

Martínez-Huitle, C. A., & Brillas, E. (2009). Decontamination of wastewaters containing synthetic organic dyes by electrochemical methods: A general review. *Applied Catalysis B: Environmental*, *87*(3–4), 105–145. https://doi.org/10.1016/j.apcatb.2008.09.017

Martínez-Huitle, C. A., Rodrigo, M. A., Sirés, I., & Scialdone, O. (2015). Single and Coupled Electrochemical Processes and Reactors for the Abatement of Organic Water Pollutants: A Critical Review. *Chemical Reviews*, *115*(24), 13362–13407. https://doi.org/10.1021/acs.chemrev.5b00361

McGriff, E. C., & McKinney, R. E. (1972). The removal of nutrients and organics by activated algae. *Water Research*, *6*(10), 1155–1164. https://doi.org/10.1016/0043-1354(72)90015-2

Mohd Udaiyappan, A. F., Abu Hasan, H., Takriff, M. S., & Sheikh Abdullah, S. R. (2017). A review of the potentials, challenges and current status of microalgae biomass applications in industrial wastewater treatment. *Journal of Water Process Engineering*, *20*(June), 8–21. https://doi.org/10.1016/j.jwpe.2017.09.006

Monlau, F., Sambusiti, C., Ficara, E., Aboulkas, A., Barakat, A., & Carrère, H. (2015). New opportunities for agricultural digestate valorization: Current situation and perspectives. *Energy and Environmental Science*, *8*(9), 2600–2621. https://doi.org/10.1039/c5ee01633a

Moradi, M., Vasseghian, Y., Khataee, A., Kobya, M., Arabzade, H., & Dragoi, E. N. (2020). Service life and stability of electrodes applied in electrochemical advanced oxidation processes: A comprehensive review. *Journal of Industrial and Engineering Chemistry*, *87*, 18–39. https://doi.org/10.1016/j.jiec.2020.03.038

Morales-Amaral, M. del M., Gómez-Serrano, C., Acién, F. G., Fernández-Sevilla, J. M., & Molina-Grima, E. (2015). Production of microalgae using centrate from anaerobic digestion as the nutrient source. *Algal Research*, *9*, 297–305. https://doi.org/10.1016/j.algal.2015.03.018

Moreira, A. S. P., Nunes, F. M., Domingues, M. R., & Coimbra, M. A. (2012). Coffee melanoidins: Structures, mechanisms of formation and potential health impacts. *Food and Function*, *3*(9), 903–915. https://doi.org/10.1039/c2fo30048f

Moretti, P., Morais de Araujo, J., Borges de Castilhos, A., Buffière, P., Gourdon, R., & Bayard, R. (2020). Characterization of municipal biowaste categories for their capacity to be converted into a feedstock aqueous slurry to produce methane by anaerobic digestion. *Science of the Total Environment*, *716*. https://doi.org/10.1016/j.scitotenv.2020.137084

Mucha, A. P., Dragisa, S., Dror, I., Garuti, M., Hullebusch, E. D. Van, Repinc, S. K., & Mun, J. (2019). Re-use of digestate and recovery techniques. In *Trace Elements in Anaerobic Biotechnologies* (pp. 181–213). IWA Publishing. https://doi.org/10.2166/9781789060225_0181

Murthy, P. S., & Madhava Naidu, M. (2012). Sustainable management of coffee industry by-products and value addition - A review. *Resources, Conservation and Recycling*, *66*, 45–58. https://doi.org/10.1016/j.resconrec.2012.06.005

Mussatto, S. I., Machado, E. M. S., Martins, S., & Teixeira, J. A. (2011). Production, Composition, and Application of Coffee and Its Industrial Residues. *Food and Bioprocess Technology*, *4*(5), 661–672. https://doi.org/10.1007/s11947-011-0565-z

Neyens, E., & Baeyens, J. (2003). A review of classic Fenton's peroxidation as an advanced oxidation technique. *Journal of Hazardous Materials*, *98*(1–3), 33–50. https://doi.org/10.1016/S0304-3894(02)00282-0

Nidheesh, P. V., & Gandhimathi, R. (2012). Trends in electro-Fenton process for water and wastewater treatment: An overview. *Desalination*, *299*, 1–15. https://doi.org/10.1016/j.desal.2012.05.011

Ou, B., Wang, J., Wu, Y., Zhao, S., & Wang, Z. (2020). Reuse of PANI wastewater treated by anodic oxidation/electro-Fenton for the preparation of PANI. *Chemosphere*, *245*. https://doi.org/10.1016/j.chemosphere.2019.125689

Özcan, A. A., & Özcan, A. (2018). Investigation of applicability of Electro-Fenton method for the mineralization of naphthol blue black in water. *Chemosphere*, *202*, 618–625. https://doi.org/10.1016/j.chemosphere.2018.03.125

Panizza, M., & Cerisola, G. (2005). Application of diamond electrodes to electrochemical processes. *Electrochimica Acta*, *51*(2), 191–199. https://doi.org/10.1016/j.electacta.2005.04.023

Panizza, M., & Cerisola, G. (2009). Direct and mediated anodic oxidation of organic pollutants. *Chemical Reviews*, *109*(12), 6541–6569. https://doi.org/10.1021/cr9001319

Pereira, G. F., El-Ghenymy, A., Thiam, A., Carlesi, C., Eguiluz, K. I. B., Salazar-Banda, G. R., & Brillas, E. (2016). Effective removal of Orange-G azo dye from water by electro-Fenton and photoelectro-Fenton processes using a boron-doped diamond anode. *Separation and Purification Technology*, *160*, 145–151. https://doi.org/10.1016/j.seppur.2016.01.029

Pinto, M. P. M., Mudhoo, A., de Alencar Neves, T., Berni, M. D., & Forster-Carneiro, T. (2018). Co–digestion of coffee residues and sugarcane vinasse for biohythane generation. *Journal of Environmental Chemical Engineering*, *6*(1), 146–155. https://doi.org/10.1016/j.jece.2017.11.064

Provasoli, L., Pintner, I. J. (1959). Artificial media for fresh-water algae: problems and suggestions. In Tryon, C. A., Jr. & Hartmann, R.T. (eds.), *The Ecology of Algae. Spec. Pub. No. 2 Edn.* (pp. 84–96). Pymatuning Laboratory of Field Biology, University of Pittsburgh, Pittsburgh.

Pulgarin, A., Kapeller, A. G., Tarik, M., Egloff, S., Mariotto, M., Ludwig, C., & Refardt, D. (2021).

Cultivation of microalgae at high-density with pretreated liquid digestate as a nitrogen source: Fate of nitrogen and improvements on growth limitations. *Journal of Cleaner Production*, *324*, 129238. https://doi.org/10.1016/j.jclepro.2021.129238

Qin, Z. Z., Chen, Y. M., & Su, C. F. (2003). The Determination of Caramel Yellow Index. *China Condiment*, *7*, 30–37.

Raheem, A., Prinsen, P., Vuppaladadiyam, A. K., Zhao, M., & Luque, R. (2018). A review on sustainable microalgae based biofuel and bioenergy production: Recent developments. *Journal of Cleaner Production*, *181*, 42–59. https://doi.org/10.1016/j.jclepro.2018.01.125

Rahman, K. M. (2019). Food and High Value Products from Microalgae: Market Opportunities and Challenges. In M. A. Alam et al. (eds.), *Microalgae Biotechnology for Food, Health and High Value Products* (pp. 3–27). Springer Nature Singapore Pte Ltd. https://doi.org/https://doi.org/10.1007/978-981-15-0169-2_1

Rajagopal, R., Mousavi, S. E., Goyette, B., & Adhikary, S. (2021). Coupling of microalgae cultivation with anaerobic digestion of poultry wastes: Toward sustainable value added bioproducts. *Bioengineering*, *8*(5), 57. https://doi.org/10.3390/bioengineering8050057

Ramsundar, P., Guldhe, A., Singh, P., & Bux, F. (2017). Assessment of municipal wastewaters at various stages of treatment process as potential growth media for Chlorella sorokiniana under different modes of cultivation. *Bioresource Technology*, *227*, 82–92. https://doi.org/10.1016/j.biortech.2016.12.037

Rigueto, C. V. T., Nazari, M. T., De Souza, C. F., Cadore, J. S., Brião, V. B., & Piccin, J. S. (2020). Alternative techniques for caffeine removal from wastewater: An overview of opportunities and challenges. *Journal of Water Process Engineering*, *35*(March). https://doi.org/10.1016/j.jwpe.2020.101231

Rodrigues, N. P., & Bragagnolo, N. (2013). Identification and quantification of bioactive compounds in coffee brews by HPLC-DAD-MSn. *Journal of Food Composition and Analysis*, *32*(2), 105–115. https://doi.org/10.1016/j.jfca.2013.09.002

Sahu, O. P., & Chaudhari, P. K. (2015). Electrochemical treatment of sugar industry wastewater: COD and color removal. *Journal of Electroanalytical Chemistry*, *739*, 122–129. https://doi.org/10.1016/j.jelechem.2014.11.037

Sánchez-Monedero, M. A., Mondini, C., De Nobili, M., Leita, L., & Roig, A. (2004). Land application of biosolids. Soil response to different stabilization degree of the treated organic matter. *Waste Management*, *24*(4), 325–332. https://doi.org/10.1016/j.wasman.2003.08.006

Santal, A. R., Singh, N. P., & Saharan, B. S. (2011). Biodegradation and detoxification of melanoidin from distillery effluent using an aerobic bacterial strain SAG 5 of Alcaligenes faecalis. *Journal of Hazardous Materials*, *193*, 319–324. https://doi.org/10.1016/j.jhazmat.2011.07.068

Sathishkumar, K., Sathiyaraj, S., Parthipan, P., Akhil, A., Murugan, K., & Rajasekar, A. (2017). Electrochemical decolorization of methyl red by RuO_2-IrO_2-TiO_2 electrode and biodegradation with Pseudomonas stutzeri MN1 and Acinetobacter baumannii MN3: An integrated approach. *Chemosphere*, *183*, 204–211. https://doi.org/10.1016/j.chemosphere.2017.05.087

Sayedin, F., Kermanshahi-pour, A., He, Q. S., Tibbetts, S. M., Lalonde, C. G. E., & Brar, S. K. (2020). Microalgae cultivation in thin stillage anaerobic digestate for nutrient recovery and bioproduct production. *Algal Research*, *47*(July 2019), 101867. https://doi.org/10.1016/j.algal.2020.101867

Sekine, M., Yoshida, A., Akizuki, S., Kishi, M., & Toda, T. (2020). Microalgae cultivation using undiluted anaerobic digestate by introducing aerobic nitrification-desulfurization treatment. *Water Science and Technology*, *82*(6), 1070–1080. https://doi.org/10.2166/wst.2020.153

Simaratanamongkol, A., & Thiravetyan, P. (2010). Decolorization of melanoidin by activated carbon obtained from bagasse bottom ash. *Journal of Food Engineering*, *96*(1), 14–17. https://doi.org/10.1016/j.jfoodeng.2009.06.033

Sirés, I., Brillas, E., Oturan, M. A., Rodrigo, M. A., & Panizza, M. (2014). Electrochemical advanced oxidation processes: Today and tomorrow. A review. *Environmental Science and Pollution Research*, *21*(14), 8336–8367. https://doi.org/10.1007/s11356-014-2783-1

Song, Y., Hahn, H. H., & Hoffmann, E. (2002). Effects of solution conditions on the precipitation of phosphate for recovery: A thermodynamic evaluation. *Chemosphere*, *48*(10), 1029–1034. https://doi.org/10.1016/S0045-6535(02)00183-2

Spolaore, P., Joannis-Cassan, C., Duran, E., & Isambert, A. (2006). Commercial applications of microalgae. *Journal of Bioscience and Bioengineering*, *101*(2), 87–96. https://doi.org/10.1263/jbb.101.87

Stengel, D. B., Connan, S., & Popper, Z. A. (2011). Algal chemodiversity and bioactivity: Sources of natural variability and implications for commercial application. *Biotechnology Advances*, *29*(5), 483–501. https://doi.org/10.1016/j.biotechadv.2011.05.016

Susanto, H., Roihatin, A., & Widiasa, I. N. (2016). Production of colorless liquid sugar by ultrafiltration coupled with ion exchange. *Food and Bioproducts Processing*, *98*, 11–20. https://doi.org/10.1016/j.fbp.2015.12.002

Thiam, A., Brillas, E., Garrido, J. A., Rodríguez, R. M., & Sirés, I. (2016). Routes for the electrochemical degradation of the artificial food azo-colour Ponceau 4R by advanced oxidation processes. *Applied Catalysis B: Environmental*, *180*, 227–236. https://doi.org/10.1016/j.apcatb.2015.06.039

Thiam, A., Sirés, I., Garrido, J. A., Rodríguez, R. M., & Brillas, E. (2015). Decolorization and mineralization of Allura Red AC aqueous solutions by electrochemical advanced oxidation processes. *Journal of Hazardous Materials*, *290*, 34–42.

https://doi.org/10.1016/j.jhazmat.2015.02.050

Tian, Y., He, W., Liang, D., Yang, W., Logan, B. E., & Ren, N. (2018). Effective phosphate removal for advanced water treatment using low energy, migration electric–field assisted electrocoagulation. *Water Research*, *138*, 129–136. https://doi.org/10.1016/j.watres.2018.03.037

Tomasik, P. (2003). CARAMEL | Properties and Analysis. In *Encyclopedia of Food Sciences and Nutrition* (Issue 2, pp. 852–858). Elsevier.

USDA (2023) Coffee : World Markets and Trade. *United States Department of Agriculture Foreign Agricultural Service*. https://www.fas.usda.gov/data/coffee-world-markets-and-trade. Accessed 22 June 2023

Vítěz, T., Koutný, T., Šotnar, M., & Chovanec, J. (2016). On the spent coffee grounds biogas production. *Acta Universitatis Agriculturae et Silviculturae Mendelianae Brunensis*, *64*(4), 1279–1282. https://doi.org/10.11118/actaun201664041279

Wang, G., Liu, Y., Ye, J., Lin, Z., & Yang, X. (2020). Electrochemical oxidation of methyl orange by a Magnéli phase Ti_4O_7 anode. *Chemosphere*, *241*, 125084. https://doi.org/10.1016/j.chemosphere.2019.125084

Wang, L., Addy, M., Liu, J., Nekich, C., Zhang, R., Peng, P., Cheng, Y., Cobb, K., Liu, Y., Wang, H., & Ruan, R. (2019). Integrated process for anaerobically digested swine manure treatment. *Bioresource Technology*, *273*(November), 506–514. https://doi.org/10.1016/j.biortech.2018.11.050

Wang, L., Li, Y., Chen, P., Min, M., Chen, Y., Zhu, J., & Ruan, R. R. (2010). Anaerobic digested dairy manure as a nutrient supplement for cultivation of oil-rich green microalgae Chlorella sp. *Bioresource Technology*, *101*(8), 2623–2628. https://doi.org/10.1016/j.biortech.2009.10.062

Wang, S. K., Stiles, A. R., Guo, C., & Liu, C. Z. (2014). Microalgae cultivation in photobioreactors: An overview of light characteristics. *Engineering in Life Sciences*, *14*(6), 550–559. https://doi.org/10.1002/elsc.201300170

Wang, Y., Zhou, C., Meng, G., Bai, J., Geng, X., LV, Y., & Chen, X. (2020). Treatment of landfill leachate membrane filtration concentrate by synergistic effect of electrocatalysis and electro-Fenton. *Journal of Water Process Engineering*, *37*(June), 101458. https://doi.org/10.1016/j.jwpe.2020.101458

Woldesenbet, A. G., Woldeyes, B., & Chandravanshi, B. S. (2014). Characteristics of wet coffee processing waste and its environmental impact in Ethiopia. *International Journal of Research in Engineering and Science*, *2*(4), 1–5. https://doi.org/ijres. 2320-9364.

Yamjala, K., Nainar, M. S., & Ramisetti, N. R. (2016). Methods for the analysis of azo dyes employed in food industry - A review. *Food Chemistry*, *192*, 813–824.

https://doi.org/10.1016/j.foodchem.2015.07.085

Yoshida, K., Yoshida, S., Seki, Y., Takahashi, T., Ihara, I., & Toyoda, K. (2007). Basic study of electrochemical treatment of ammonium nitrogen-containing wastewater using boron-doped diamond anode. *SEI Technical Review*, *65*, 71–73.

Yoshida, S., Kobayashi, Y., & Nakashima, T. (2014). Electrochemical Property of Diamond Enhanced with Boron Doping, and its Application. *Journal of Smart Processing*, *3*(6), 346–353. https://doi.org/10.7791/jspmee.3.346

Zhang, H., Fei, C., Zhang, D., & Tang, F. (2007). Degradation of 4-nitrophenol in aqueous medium by electro-Fenton method. *Journal of Hazardous Materials*, *145*(1–2), 227–232. https://doi.org/10.1016/j.jhazmat.2006.11.016

Zhang, T., Tonouchi, K., Kong, Z., Li, Y., Cheng, H., Qin, Y., & Li, Y. Y. (2021). Improvement of coffee grounds high solid thermophilic methane fermentation by co-digestion with in-situ produced waste activated sludge: Performance and stability. *Science of the Total Environment*, *765*, 142551. https://doi.org/10.1016/j.scitotenv.2020.142551

Zheng, Y., Li, T., Yu, X., Bates, P. D., Dong, T., & Chen, S. (2013). High-density fed-batch culture of a thermotolerant microalga chlorella sorokiniana for biofuel production. *Applied Energy*, *108*, 281–287. https://doi.org/10.1016/j.apenergy.2013.02.059